Journal of Materials Chemistry B

Accepted Manuscript

ROYAL SOCIETY OF CHEMISTRY

www.rsc.org/materialsB

Amelogenin and Enamel Biomimetics

Qichao Ruan and Janet Moradian-Oldak *

Center for Craniofacial Molecular Biology, Herman Ostrow School of Dentistry,

University of Southern California, Los Angeles, CA 90033, USA

* Corresponding author. Tel.: +1 323 442 1759; fax: +1 323 442 2981.

Email address: joldak@usc.edu (J. Moradian-Oldak).

Keywords:

Amelogenin, self-assembly, enamel, biomineralization, apatite, biomimetic, enamel reconstruction

Janet Moradian-Oldak is a professor at the Division of Biomedical Sciences, Herman Ostrow School of Dentistry with a joint appointment in the Biomedical Engineering Department at the USC Viterbi School of Engineering. The main objective of her research is understanding the principles that govern the biomineralization of dental enamel by learning how the intricate matrix of proteins, enzymes and minerals come together to form this remarkable bioceramic. The ultimate goal is to develop new dental materials that more closely mimic the structure and function of natural tooth enamel. Her work has resulted in two US patents and more than 100 articles and book chapters.

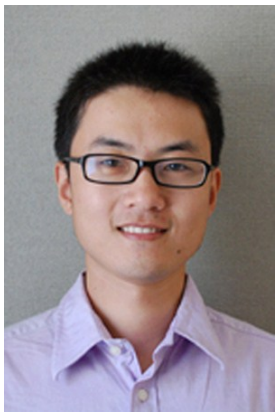

Qichao Ruan received his Ph.D. in Materials Science form the Shanghai Institute of Ceramics, Chinese Academy of Sciences (SICCAS) in 2011, under the supervision of Prof. Yingchun Zhu. Since then, he has been working as a postdoctoral researcher in the group of Prof. Janet Moradian-Oldak at the Center for Craniofacial Molecular Biology of the University of Southern California. He has wide research interest in developing biomimetic materials and nanosturctures for biomedical application.

Abstract

Mature tooth enamel is acellular and does not regenerate itself. Developing technologies that rebuild tooth enamel and preserve tooth structure is therefore of great interest. Considering the importance of amelogenin protein in dental enamel formation, its ability to control apatite mineralization *in vitro,* and its potential to be applied in fabrication of future bio-inspired dental material this review focuses on two major subjects: amelogenin and enamel biomimetics. We review the most recent findings on amelogenin secondary and tertiary structural properties with a focus on its interactions with different targets including other enamel proteins, apatite mineral, and phospholipids. Following a brief overview of enamel hierarchical structure and its mechanical properties we will present the state-of-the-art strategies in the biomimetic reconstruction of human enamel.

1 Introduction

The protein-mediated biomineralization in biological tissue is a great source of inspiration for the engineering of advanced materials.[1-7] The biomaterials in mineralized tissues are generally optimized for their function through precise control over the structure, size, shape, and hierarchical assembly of the component parts and can be superior to many synthetic materials.[3, 4] Enamel is a highly mineralized tissue that protects the mammalian tooth from external physical and chemical damage. Mature enamel is acellular and composed of 95-97% mineral by weight with less than 1% organic material.[2, 8] The fluoridated carbonate-apatite nanocrystals found in enamel are tightly packed and arranged into an intricate interwoven structure. This organized hierarchical microstructure provides enamel with increased hardness and resistance to fracture compared to monolithic hydroxyapatite.[9] The high degree of mineralization makes enamel a fascinating model for understanding fundamental mechanisms of protein-mediated mineralization, which could be utilized by scientists for development and design of biomimetic materials with potential for application in biomedicine, dentistry and industry.[2]

The enamel formation (amelogenesis) involves a series of highly regulated cellular activities and protein-controlled mineralization processes. The generally recognized stages of enamel development are the presecretory, secretory, transitional, and maturation stages which are defined by the morphology and function of ameloblasts.[10, 11] The ameloblasts are a single cell layer that covers the developing enamel and is responsible for the enamel composition and hierarchical structure. The dynamic process of enamel biomineralization occurs in the extracellular space between the presecretory ameloblasts and the mineralized dentin.[8] Enamel crystallites initiate at the dentino-enamel junction (DEJ) immediately following fenestration and removal of the basement membrane beneath fully differentiated pre-ameloblasts.[12] After establishing the DEJ and mineralizing a thin layer of aprismatic enamel, ameloblasts develop a secretory specialization, or Tomes' process.[12] The extracellular protein matrix is continuously secreted and processed in a stepwise and controlled manner during the secretory stage, when enamel crystals grow primarily

in length and the enamel layer thickens. Once the full thickness of the enamel layer is achieved the transition and maturation stages begin. The protein matrix is proteolytically degraded during the maturation stage as crystals grow mainly in width and thickness, and is eventually removed from the extracellular space to allow completion of mineralization.[13] These orchestrated cellular and biochemical activities result in the formation of a highly mineralized and hierarchically structured biological material.

The enamel matrix proteins play vital roles in the regulation of mineralization and crystal organization during enamel development. Amelogenin is the most abundant protein in the forming enamel, constituting more than 90% of the extracellular organic matrix.[14] This protein is required for proper enamel development, as indicated by genetically engineered amelogenin-null mice, which display distinctly abnormal teeth with disorganized hypoplastic enamel.[15] The amelogenin-null enamel phenotype reveals that amelogenin is essential for the organization of the prismatic pattern, control of crystal size and regulation of elongated crystal growth and enamel thickness.[15, 16]

Proposed molecular mechanisms for the amelogenin-regulated apatite mineralization in enamel formation include two different theories. The classical theory postulates that amelogenin and its isoforms bind specifically and selectively to the crystal sides, inhibiting ion deposition on these facets and permitting crystal growth only in length during the secretory stage and in thickness during the maturation stage.[14, 17, 18] In the non-classical theory, a pathway of crystallization was suggested in which amelogenin interacts with noncrystalline calcium phosphate to form, stabilize and assemble intermediate pre-nucleation clusters that further transform into organized apatite crystals.[19-21] In addition to amelogenin, lesser amounts of other enamel proteins, such as enamelin, ameloblastin and proteinases, have also shown to be critical for normal enamel formation. These enamel matrix proteins control the initiation, habit, orientation and organization of enamel crystals in a cooperative manner and then are gradually degraded and removed during enamel maturation.[8]

Mature enamel is acellular and does not resorb or remodel. As a result, following failure enamel regeneration cannot occur *in vivo* and is therefore an attractive target for future biomimetic therapeutic approaches. Understanding these protein-mediated enamel mineralization processes can provide the knowledge and scientific tools needed for the design of biomimetic systems for promotion of enamel regrowth *in situ*.

Numerous recent reviews and book chapters summarize the function of extracellular matrix proteins in the process of enamel formation.[8, 22, 23] Excellent reviews of the historical and chronological advancement of amelogenin biochemistry and genetics are available.[14, 24, 25] The concept of enamel biomimetics was introduced in 1997 [5] and different aspects of enamel bio-inspired material synthesis have been reviewed by various investigators.[2, 4, 26] Considering the importance of amelogenin in enamel formation, its ability to control apatite mineralization *in vitro* [18, 20, 21] and its potential to be applied in fabrication of future bio-inspired material,[4] this review focuses on two major subjects: amelogenin and enamel biomimetics. We first review the most recent findings on amelogenin secondary and tertiary structural properties with a focus on its interactions with different targets such as other enamel proteins, minerals, and phospholipids. Following a brief overview of enamel hierarchical structure and its mechanical properties we will present the state-of-the-art strategies in the biomimetic reconstruction of human tooth enamel and the application of amelogenin protein in preparing such materials.

2 Amelogenin and its targets

2.1 Amelogenin structural adaptability

The most recent structural studies highlight a unique characteristic of amelogenin protein, namely the tendency to adopt a structure that fits its environment (Table 1, Fig. 1). The primary structure of amelogenin has a hydrophobic-hydrophilic polarity that might determine its ability to assemble in different modes depending upon the conditions surrounding the macromolecule.[8, 14, 27, 28]

The sequence of amelogenin is typically divided into three prominent amino acid domains: a hydrophobic tyrosine-rich N-terminal domain, called the tyrosine-rich amelogenin peptide (TRAP);[29] the central proline-rich region, which is hydrophobic and primarily composed of X-Y-proline (where X and Y are often glutamine) repeat motifs; and the hydrophilic C-terminal domain. The N- and C-terminal region amino acid sequences are highly conserved among mammalian species, suggesting that these segments play important roles in enamel development and mineralization.[30] In the following sections, we will demonstrate how amelogenin interacts with different targets mainly via these N- and C-termini (Table 1). The native amelogenin contains a single phosphate group on serine-16 that is presumed to be involved in amelogenin-calcium phosphate interactions and contribute to the ability of amelogenin to stabilize the precursor amorphous calcium phosphate.[31]

The primary sequence is enriched with disorder-promoting residues, such as Pro (P), Gln (Q), Glu (E), Arg (R), and Lys (K), leading to the intrinsically labile nature of the protein.[32, 33] Bioinformatics and experimental studies in our laboratory have demonstrated that amelogenin belongs to the class of intrinsically disordered or unstructured proteins (IDPs).[27] Unlike folded proteins, IDPs lack regular secondary or tertiary structure but are capable of transforming into a folded state following interactions with their targets and as part of their overall function.[34] Structural studies through circular dichroism (CD) and solution NMR have revealed that recombinant porcine amelogenin (rP172) exists in an extended, unfolded state in the monomeric form under acidic aqueous conditions.[27] Although the protein was reported to be globally unfolded, the presence of several short structure regions (α-helix, extended β-strand, turn/loop, and polyproline type II (PPII) conformation) was detected, hinting at the potential of this protein to recognize different interacting targets (Table 1, Fig. 1). Such interactions were proposed to serve several functional roles within the enamel extracellular matrix during the dynamic process of enamel biomineralization.[27] For example, the unfolded N-terminal TRAP domain (self-assembly A domain) offers sufficient molecular contacts for assembly within the protein-protein

interaction process.[35, 36] The tri-tyrosine motif (P**Y**PS**Y**G**Y**EPMGGW) in this N-terminal region has also been reported to have lectin-like properties (high affinity to N-acetyl D-Glugosamine), increasing the ability of amelogenin to interact with other enamel matrix glycoproteins or the cell surface glycocalyx.[37, 38] The randomly coiled structure of the C-terminal domain would provide enhanced multiple charged contacts with the mineral surface.[27] Regions close to the C-terminal have also been identified as being involved in amelogenin self-assembly (self-assembly B-domain).[39]

We have proposed that the extended and flexible structure is an important feature that facilitates the assembly of amelogenin into different quaternary structures as well as its interactions with other matrix proteins or biominerals.[27] The labile conformation provides amelogenin with structural adaptability in response to various potential enamel matrix targets. Our most recent NMR study using "solvent engineering" techniques confirmed that both the N- and C- termini of amelogenin are conformationally responsive to the structure-inducing solvent 2,2,2-trifluoroehanol (TFE) and represent potential sites for amelogenin-target interaction during enamel matrix mineralization. As it is evident from the change in CD spectra TFE induced significant increase in alpha-helical content of recombinant amelogenin rP172 (Fig. 2).[40] Based on the PPII propensity scale for individual amino acid residues, we previously reported that PPII is the dominant structure in the central region of amelogenin[33] and our solvent engineering studies confirmed that the Pro, Gln central domain is resistant to folding.[40] The rigidity in the central region and flexibility at the N- and C- termini may have important functional significance for amelogenin *in vivo*.[40]

To further evaluate structural adaptability of amelogenin we have recently analyzed the structural behavior of amelogenin in the presence of sodium dodecyl sulfate (SDS), which has the ability to mimic biological cell membranes by forming amphiphilic micelles.[41] NMR spectroscopy and structural refinement calculations using CS-Rosetta modeling confirmed that the highly conserved N-terminal domain of amelogenin was prone to forming helical structure

when bound to SDS micelles (Fig. 3). These findings revealed that significant changes in the secondary structure of amelogenin occurred upon treatment with SDS. These interactions may reflect the physiological relevance of the flexible nature of amelogenin and its sequence-specific helical propensity, which might enable it to structurally adapt when bound to targets.

2.2 Self-assembly of amelogenin

The strong tendency of amelogenin to aggregate has been known since 1960's.[42] We now have increasing evidence that amelogenin self-assembles into quaternary structures under a variety of conditions *in vitro*. These include nanospheres (Fig. 4A), nanochains (Fig. 4B), oligomers (Fig. 4C), microribbons and nanoribbons (Fig. 4D).[43-46] Self-assembly of amelogenin is sensitive to pH, protein concentration, temperature and ionic strength,[31] and also can be affected by the presence of proteases,[47] other enamel proteins, calcium phosphate ions,[45] solvent hydrophobicity and charged surfaces such as apatite minerals.[48] A single phosphorylated serine present in the sequence might have a subtle influence on amelogenin self-assembly.[49]

Earlier studies showed that the full-length recombinant amelogenin molecules can spontaneously self-assemble into nanospheres under pH = 8 conditions in the absence of calcium-phosphate.[36, 46, 50-53] We have suggested that the nanospheres were formed through intermolecular hydrophobic interactions when the hydrophilic segment of each molecule was exposed on the surface of the nanospheres.[8] The nanospheres were then proposed to be the basic structural entities of the developing enamel extracellular matrix and to play a crucial function in enamel biomineralization.[52]

The original AFM images of amelogenin nanospheres were based on samples that were processed using Karnovsky fixative [46] to prevent them from collapsing or disintegrating (Fig. 4A). While the size distribution was heterogeneous at low protein concentrations, at higher concentrations (100-300 μg/ml) particles ranging from 10 to 25 nm in diameter were detected under the AFM. It is now acceptable that nanospheres are not rigid structures and can disassemble if adsorbed onto surfaces with different hydrophobicity or different charges.[48] The formation of

do-decamers as basic subunits of nanospheres at pH 8 was illustrated by single-particle reconstruction of cryo-TEM images (Fig. 4 C).[44]

Our analyses of the particle size distribution of amelogenin assemblies in solution have suggested the existence of substructures such as monomers and discrete oligomers prior to nanosphere formation in solution (Fig. 5).[54] The formation of oligomers as the basic subunits of the typical nanospheres was also observed by transmission electron microscopy.[43] Dissecting the nanospheres by reducing the pH to 3.5 or 5.5 allowed us to better understand the chemical interactions responsible for amelogenin assembly/aggregation in the absence of calcium phosphate ions. Partial deprotonation of histidine residues at pH 5.5 resulted in the formation of oligomers, via N-terminally mediated intermolecular interactions. At pH 8, when the histidine residues are completely deprotonated, hydrophobic forces are enhanced to bind the oligomers together in the form of a nanosphere. Our recent CD analysis has revealed that while oligomer formation accompanies conformational changes in amelogenin, little structural change occurs as a result of nanosphere formation.[54] In their NMR studies, Lu *et al.* [55] reported a lack of conformational changes in amelogenin nanospheres during gel formation. We have reported that amelogenin oligomer formation *in vitro* is mediated by N-terminal protein-protein interactions and assembly, while nanosphere formation is mainly regulated by hydrophobic interactions via the histidine-rich central portion.[54] The question is whether the amelogenin oligomers (R_H = 7.5 nm) are the functional entities in enamel formation and that the nanospheres (R_H = 14nm) are simply the result of aggregation of oligomers. Particles of 15-20 nm in diameter detected by TEM are the oligomeric structures that were detected in between enamel crystallites.[52, 56] Oligomeric structures can also be stabilized under neutral conditions and in the presence of an acidic protein, namely 32 kD enamelin (section 2.4). Fluorescence experiments with single-tryptophan amelogenins revealed that upon oligomerization the C terminus of amelogenin (around residue Trp161) is exposed at the surface of the oligomers, whereas the N-terminal region around Trp25 and Trp45 is involved in protein-protein interaction.

Amelogenin has shown a tendency to further assemble into higher-order structures *in vitro*. Nanochain assemblies of amelogenin were observed in a number of studies (Fig. 4B).[20, 43, 57, 58] It was suggested that the nanochain structures were formed through further association of the amelogenin nanospheres (or association of amelogenin oligomers).[43] The bipolar nature of the molecule can facilitate the formation and/or reorganization of the chain structures.[43] Li *et al.*[57] studied the kinetics of amelogenin nanochain formation via a Brownian dynamics simulation of both translational and rotational motions. Their simulations showed a hierarchical self-assembly process in which the molecules aggregate to form oligomers and nanospheres, and the assembly of the nanospheres then leads to the formation of nanochains, in agreement with experimental findings.

The idea that oligomeric, dimeric, or even monomeric structures might be functional components during enamel formation was proposed by Shaw *et al.*,[59] who demonstrated that nanospheres can disassemble following their adsorption onto surfaces. Chen *et al.* [48] then reported that the self-assembly of amelogenin can be dramatically different on substrates and depends upon the charge of the interacting surfaces. These studies have important implications because amelogenin may be in contact with charged surfaces such as mineral and cell membranes *in vivo*.

As opposed to the previously proposed nanochain model, He *et al*.[58] reported the formation of amelogenin nanoribbons in an emulsion oil-water system. They proposed an alternative model for the protein-mediated enamel biomineralization based on parallel alignment and extension of ribbons. Nanoribbons also form in the presence of calcium phosphate under low pH conditions (pH 4-6) and stay stable for three days when exposed to neutral pH (Fig. 4D).[45, 58, 60] Histidine protonation was proposed to play an important role in providing the binding sites for phosphate bridging and formation of elongated dimers.[45]

While the ability of amelogenin to self-assemble to a variety of quaternary structures has been well documented *in vitro*, a clear model for *in vivo* functional entities of amelogenin is still lacking and requires further investigation. It is noteworthy that amelogenin molecules do not

occur in isolation *in vivo*, so the presence of other components such as mineral, other proteins, cell surface and lipoid particles needs to be considered.

2.3 Amelogenin-mineral interactions

Experimental evidence that amelogenin interacts with apatite crystals was documented in studies of seeded crystal growth and analytical evaluation of adsorption affinity.[61-63] Removal of the hydrophilic C-terminal significantly decreased amelogenin affinity to apatite crystals.[64, 65] Direct evidence for the orientation of the charged C-terminal region near the apatite crystal surface was provided by solid state NMR and neutron scattering as well as computational methods.[66, 67] The C-terminal portion has a significantly higher affinity for binding to the (100) side face of apatite compared to the cross section (001) face, a finding that might explain the c-axial elongated growth of enamel apatite crystals.[68] Amelogenin can also interact with the apatite surface through the N-terminal region, as isolated peptides from the N-terminal were detected to be bound after proteolytic digestion of full-length amelogenin in the presence of apatite.[69] Although serine phosphorylation is not required for the binding of amelogenin LRAP (Leucine Rich Amelogenin Polypeptide) to apatite, the N-terminal binding was stronger when the ^{16}Ser was phosphorylated.[70-72] Lu *et al.*[55] found that regions of amelogenin that appear to be primarily random coils in the nanosphere-gel adopt a β-strand structure and are less mobile after HAP binding, indicative of a structural switch upon binding that may be important to the role of amelogenin in enamel development (Table 1). The binding of LRAP to apatite promotes folding of domains at both the C- and N-terminal regions, promoting a conformational transition from random coil to extended beta strand at the C-terminal, and partial alpha helix at the N-terminal.[55, 70, 73] LRAP-bound apatite is mostly extended, thereby covering the apatite surface efficiently (Fig. 6).

Specific roles for amelogenin in nucleation, growth, regulation of crystal size and shape, and control of crystal-crystal aggregation have been proposed.[26, 74-76] Studies of the kinetics of crystal nucleation *in situ* and in real time using a quartz crystal microbalance (QCM) showed that

recombinant amelogenin reduced the induction time for nucleation compared to solutions without protein.[74] Wang *et al.* [76] reported that amelogenin dramatically accelerates the nucleation kinetics by decreasing the induction time in a dose-dependent manner in a controlled constant-composition *in vitro* crystallization system. An interfacial structural match between amelogenin assemblies (mainly oligomers) and Ca-P nanoclusters was proposed. Considering the ability of amelogenin assemblies to reduce the interfacial energy needed for nucleation of hydroxyapatite, it is not surprising that apatite nucleation is promoted by this protein in *in vitro* model systems. However, there is no direct evidence that enamel mineralization occurs *in vivo* via amelogenin-mediated heterogeneous nucleation. In particular, the observation that the enamel mineralization still occurs in amelogenin null mice does not support a direct nucleating function for amelogenin *in vivo*.[15]

The classical theory of crystallization in amelogenesis postulates that extracellular matrix proteins shape crystallites by specifically inhibiting ion deposition on the crystal sides, orient them by binding multiple crystallites and establish higher levels of crystal organization. Numerous *in vitro* experiments have been conducted to support the classical theory and to investigate the amelogenin-crystal interaction.[17, 18, 77-82] These studies suggested that amelogenin specifically and selectively adsorbs to crystal faces to direct growth only in the *c*-axis direction. For example, amelogenin was found to interact most strongly with the (010) face, followed by the (001) and then (100) faces of OCP, explaining the elongated growth and increase of the thickness-to-width ratio. Nevertheless, it is still questionable whether the classical theory can explain how enamel forms naturally.[83]

In the last decade an increasing number of studies have proposed a non-classical pathway of crystallization for enamel mineralization, which involves a co-assembly of amelogenin and the transient mineral phases.[20] The presence of transient mineral phases in developing enamel has been suggested in several *in vivo* studies.[84-86] Beniash *et al.* [19] characterized the forming enamel mineral during the early secretory stage as amorphous calcium phosphate, which eventually

transforms into apatite crystals. It has been further suggested that the mineral morphology and organization in enamel are determined prior to its crystallization.[19] While this might be a reasonable explanation for the early stage of enamel crystal formation, the eventual ribbon-shaped morphology of enamel crystals cannot be easily explained due to the dynamic processing of enamel matrix during the maturation stage when the crystals mainly grow in thickness and width.

It is speculated that amelogenin transiently stabilizes amorphous calcium phosphate (ACP) and regulates the formation of parallel arrays of mineral crystals. The native phosphorylated amelogenin has been found to stabilize ACP for extended periods of time. By investigating the amelogenin-mediated crystallization in a constant composition (CC) crystallization system, Yang *et al.* [21] suggested a nucleation model in which amelogenin was proposed to stabilize the pre-nucleation Ca-P clusters and mediate their aggregation to form the oriented and elongated organized crystals (Fig. 7). In this model, two stages are proposed in the process of amelogenin-mediated apatite mineralization: (i) controlled aggregation of the Ca-P nanoclusters and (ii) organized postnucleation crystal growth involving a stepwise hierarchical co-assembly of Amel−Ca−P nanoclusters. Hierarchical co-assembly of Amel−ACP particles gives rise to a remarkably high degree of cooperativity at low driving force. Under cooperative kinetic control, the co-assembly of Amel−Ca−P clusters plays an explicit role in directing Amel/ACP nanoparticles toward the final elongated crystalline structure.[21]

The formation of the primary building blocks (nanocluster composites) probably imparts kinetic and thermodynamic stability to the system, which may lower the free-energy barrier to formation of secondary structures of intermediate phases (Amel/ACP nanosphere chains and nanorods), which ultimately undergo phase transformation to form the final crystalline phase of mature enamel (elongated HAP). Numerous *in vitro* experiments provide evidence for the function of amelogenin in the non-classical crystallization of enamel crystals;[44] however,

additional studies are needed to identify the pre-nucleation clusters *in vivo* and clarify their role in enamel mineralization.

2.4 Amelogenin-enamelin interactions

Another potential target for amelogenin is the least abundant (3-5%) acidic phosphorylated glycoprotein enamelin. It is believed that interactions between amelogenin and enamelin play a vital role in controlling enamel crystal formation.[8] The importance of enamelin in dental enamel formation has been demonstrated unequivocally by various *in vivo* studies.[87-90] In enamelin null mice, a true enamel layer was not formed.[12, 89, 90] Among the different enamelin cleavage products, the 32 kDa enamelin is the most stable fragment and is highly conserved among species, suggesting that it plays a critical functional role in enamel formation.[91, 92]

Enamelin in cooperation with amelogenin promoted the kinetics of apatite nucleation in a dose-dependent manner.[93] We have also demonstrated the cooperative regulatory action of the 32 kDa enamelin and amelogenin on the growth morphology of octacalcium phosphate (OCP) crystals.[94, 95] Adding enamelin to the amelogenin "gel-like matrix" resulted in an obvious increase in the length-to-width ratio (aspect ratio) of OCP crystals in a dose-dependent manner. Moreover, the presence of enamelin in the amelogenin matrix enhanced the stability of the transient amorphous calcium phosphate (ACP) phase.[94] It was proposed that the cooperative effect of enamelin and amelogenin was attained through co-assembling of enamelin and amelogenin.

Enamelin has been shown to interact directly with amelogenin, changing its conformation (Fig. 8), stabilizing the oligomers, and partially dissociating amelogenin nanospheres.[96,97] The 32 kDa enamelin has the potential to interact with both full-length and truncated amelogenin lacking the C-terminal through the tyrosyl motif at the N-terminal.

We recently analyzed the co-localization between enamelin and amelogenin in postnatal day 1-8 mandibular mouse molars using dual-color confocal microscopy.[98] The results showed that amelogenin and enamelin are secreted into the extracellular matrix on the cuspal slopes of the molars at day 1 and that secretion of both proteins continues to at least day 8. At day 8 enamelin

and amelogenin co-localize near the secretory face of the ameloblasts. The degree of co-localization decreases as the enamel matures, both along the secretory faces of the ameloblasts and throughout the entire thickness of the enamel. The finding that enamelin and amelogenin co-localize *in vivo* further supports our hypothesis that they cooperate to control crystal formation, particularly at the beginning of enamel formation.

2.5 Amelogenin-ameloblastin interactions

Ameloblastin is considered critical for proper enamel formation because a true enamel layer fails to appear on the teeth of ameloblastin mutant mice.[99-101.]

A recent study showed that amelogenin-ameloblastin double knock-out mice have additional enamel defects not observed in either amelogenin knock-out or ameloblastin knock-out mice,[102] lending support to the notion that amelogenin and ameloblastin interact and have synergistic roles in enamel development. The co-distribution of amelogenin and ameloblastin in the majority of the secretory granules in Tomes' processes during appositional growth of the enamel layer may reflect a form of functional association between these two distinct proteins.[101] Ameloblastin is therefore another potential target for amelogenin.

Ameloblastin is the second most abundant enamel matrix protein after amelogenin.[91, 103, 104] It is secreted together with amelogenin and rapidly processed after secretion. The hydrophobic N-terminal cleavage products accumulate in the “sheath” space throughout the enamel layer while the calcium-binding C-terminal cleavage products are on the rods and are not detectable beyond a depth of 50 μm from the surface of the newly formed enamel.[13, 105]

The first *in vitro* evidence of interactions between amelogenin and ameloblastin was provided a decade ago and revealed that these interactions may occur via the lectin-like binding domain of amelogenin.[106] In our most recent CD spectra analysis of ameloblastin in the presence of equimolar amelogenin we demonstrated that amelogenin induced changes in the secondary structure of ameloblastin, increasing alpha helical context (Fig. 9). The structural changes in

ameloblastin at this low amelogenin concentration was a strong support for the notion that the proteins formed hetero-assemblies.

In vivo evidence of co-localization of ameloblastin with amelogenin was provided using immune histochemical methods.[107] Quantitative co-localization analysis along the secretory faces of ameloblasts using antibodies against the N-terminal and C-terminal of ameloblastin revealed that at day 1, very high percentages of both the ameloblastin and amelogenin co-localized. Analysis of the entire thickness on day 8 revealed no significant co-localization of amelogenin with the C-terminal of ameloblastin in the bulk of enamel, but a low level of co-localization was detected with the N-terminal of ameloblastin. With the progress of amelogenesis and as ameloblastin and amelogenin degradation progressed, co-localization pattern changed as following: (i) there was a segregation in distribution of ameloblastin C- and N-terminal, (ii) co-localization of amelogenin with the C-terminal of ameloblastin decreases while co-localization of amelogenin with the ameloblastin N-terminal did not change. Amelogenin and N-terminal ameloblastin co-localized in the "sheath" space.[107] (P.Mazumder, S.Parapajari and J.Moradian-Oldak, in preparation.) Our data suggest that amelogenin-ameloblastin complexes may be the functional entities not only at the early stage of enamel mineralization but also later during maturation.

2.6 Amelogenin-phospholipid interactions

We recently explored interactions between amelogenin and liposomes in order to shed light on the mechanisms of amelogenin-cell interactions during amelogenesis. Amelogenin proteins are synthesized by the ameloblasts and secreted via matrix secretory vesicles. Moreover, interactions between enamel extracellular matrix components and ameloblasts might be of great importance for polarization, differentiation or migration of ameloblasts during the dynamic process of amelogenesis.[108]

We applied fluorescence spectroscopy, CD, NMR and DLS to investigate binding between recombinant amelogenin rP172 with negatively-charged (POPG)[1] and zwitterionic (POPC)[2] small unilamellar vesicles as model membranes. We prepared a mixture of different lipids to mimic the apparent lipid composition of the ameloblast membrane, called ACML[3]. We demonstrated that amelogenin has the ability to interact with zwitterionic and negatively charged liposomes via electrostatic as well as hydrophobic interaction.[109]

Adding negatively-charged small unilamellar vesicles to monomeric amelogenin at pH 3.5 resulted in greater burial of the Trp residues of rP172, and the hydrophobic membrane environment of the phospholipids induced a structural transition of rP172 from random coil to alpha helix. NMR studies revealed conformational changes and alterations in backbone dynamics within the amelogenin molecule, and suggested that such changes may be concentrated at the N- and C-termini (Table 1).

Under more physiologically relevant pH conditions (pH 8.0), where amelogenin forms nanospheres, the wavelength of the maximal intrinsic fluorescence emission is 15 nm shorter than at pH 3.5 because the Trp residues are in a more hydrophobic environment. At pH 8.00, amelogenin interactions with negatively charged lipid vesicles were weak and did not show a blue shift in the fluorescence spectra. However, quenching experiments and drawing the Stern-Volmer plots indicated that rP172 interacted with lipid vesicles. Interestingly, the ANS fluorescence decreased upon interaction of rP172 with anionic lipid vesicles, confirming that nanospheres disassembled upon interaction with the lipids. A systematic analysis of four mutant amelogenins, in each of which only one Trp residue was present and behaved precisely in the same way as the wild-type, we were able to show that amelogenin possesses membrane-binding ability mainly via its N-terminal close to residues W25 and W45 (S. Bekshe Lokappa, K. Balakrishna Chandrababu,

[1] 1-palmitoyl-2-oleoyl-sn-glycero-3-phosphoglycerol
[2] 1-palmitoyl-2-oleoyl-sn-glycero-3-phosphocholine
[3] ACML, ameloblast cell membrane-mimicking lipid vesicles

and J. Moradian-Oldak, in preparation). A disordered-to-ordered conformational change was observed based on CD and NMR studies (Table 1).

2.7 Amelogenin-MMP-20 interactions

During enamel formation, amelogenin and other enamel proteins are cleaved by proteinases after they are secreted and further degraded during the early maturation phase, allowing the enamel layer to achieve a high degree of mineralization.[13] Two major proteinases, matrix metalloproteinase-20 (MMP-20, also known as enamelysin) and serine proteinase kallikrein-4 (KLK-4), have been described. Generally, during the secretory stage, MMP-20 cleaves the amelogenin and other proteins into a number of stable intermediate products, while during the maturation stage, KLK-4 degrades and eventually removes the protein matrix in a specific and timely manner.

The full-length amelogenin is first cleaved by MMP-20 at the hydrophilic C-terminus, followed by the N-terminus. The interaction of amelogenin with MMP-20 is of a particular interest as the most prominent interacting domains are gradually removed by MMP-20. The action of MMP-20 on amelogenin therefore can affect its interactions with all of the aforementioned targets (sections 2.2-2.6).

In light of these amelogenin-MMP-20 interactions, MMP-20 was proposed to: (i) control amelogenin self-assembly, (ii) decrease amelogenin-apatite binding affinity, (iii) control ACP to apatite phase transformation by amelogenin,[110] and/or (iv) prevent unwanted protein occlusion inside apatite crystals.[111]

It has been proposed that control of the protein self-assembly process by MMP-20 allows the programmed and elongated growth of apatite crystals in a hierarchically organized manner. Nanorod structures can be formed *in vitro* by means of co-assembly of amelogenin and its cleavage products during a comparatively slow proteolysis process.[47] The proteolytic activities of MMP-20 also affect amelogenin-apatite interactions by producing intermediate products that have less affinity for apatite and can affect OCP crystal morphology in different ways.[17, 65, 69]

The idea that MMP-20 prevents unwanted amelogenin occlusion inside growing crystals was recently tested utilizing calcite as a mineral system.[111] It was found that recombinant porcine amelogenin (rP172) could alter the shape of calcite crystals and became occluded inside the crystals. In contrast, the occlusion of amelogenin into the calcite crystals was drastically decreased in rP172-rhMMP-20 samples. Truncated amelogenin lacking the hydrophilic C-terminal and the 25-residue C-terminal domain alone produced crystals with regular shapes and less occluded organic material. Based on these *in vitro* observations, we suggested that removal of the C-terminus by MMP-20 diminishes the affinity of amelogenin to the crystals, and therefore prevents occlusion of amelogenin into them. The concept that MMP-20 prevents occlusion of amelogenin in calcium phosphate crystals was been examined and demonstrated using brushite crystals as a model system (Ren *et al.*, in preparation). Systematic analysis of occluded proteins in MMP-20 knockout and wild-type mice is currently ongoing to unequivocally confirm this hypothesis (Parjapati *et al.*, in preparation).

3 Enamel and its biomimetics

Dental enamel is a masterpiece among bioceramics and the hardest material found in mammals. The unique mechanical properties of enamel enable it to perform the functions of incision, laceration, and grinding of food during mastication.[112] It also faces the lifelong challenge of maintaining robust mechanical performance in a bacteria-filled environment.[2] Additionally, mature enamel is acellular and does not regenerate after substantial mineral loss, which often occurs as dental caries or erosion as well as due to congenital malformation, trauma or mastication.

The established way to treat initial carious lesions and submicrometer erosive is the application of remineralizing agents. Oral healthcare products containing fluoride or casein phosphopeptide-amorphous calcium phosphate (CPP-ACP) are effective in re-mineralizing enamel but none of these commercially available products have the potential to promote the formation of organized apatite crystals.[113, 114] The conventional treatments for deep enamel cavities involve mechanical

drilling and subsequent filling with artificial materials such as amalgam, ceramic or composite resins. However, even after those treatments secondary caries often arises at the interface between the original enamel and the filling materials due to weakening adhesion over time. As a result, a synthetic enamel-like material with a robust adhesion to the enamel is an attractive target for future biomimetic and therapeutic approaches.

Biomimetic strategy for enamel repair may offer an ideal solution when organized enamel apatite crystals with robust attachment to the enamel surface can be grown.[115] Such strategy will lead to development of a strong material and will eliminate the problem of secondary caries. As discussed in the previous section, amelogenin plays a critical role in enamel formation and has a great potential to develop the biomimetic systems for enamel repair. Therefore, following a brief description of enamel microstructure and mechanical properties, this section of the review focuses on the biomimetic reconstruction of human tooth enamel with an emphasis on the amelogenin-containing system.

3.1 Enamel microstructure and mechanical properties

It is generally recognized that the mechanical response of enamel depends upon its unique architecture and mineral/organic composition. Understanding the enamel microstructure and associated mechanical properties could therefore motivate engineering of more robust dental materials as well as inspire fabrication of non-biological materials.

Enamel contains structures at different hierarchical levels from the nanoscale to microscale (Fig.10).[2, 116] On the nanoscale level, the basic elements of mature enamel are highly organized, hydroxyapatite crystallites that are parallel to their *c*-axis with dimensions of 50-70 nm in width, 20-35 nm thickness and with an aspect ratio greater than 1000 (Fig. 10A-C).[8] The thickness of the enamel crystallites increases from the DEJ towards the outer layer.[117, 118] On the microscale, these crystallites are grouped into more complex, micrometer-sized structures known as rods (prisms) and interrods (interprismatic substance), which are regarded as the fundamental organizational units of mammalian enamel (Fig. 10D). At the boundary between the rod and interrod enamel is a

narrow space containing organic material so-called "rod sheath" material. The sizes of the rods and interrods vary depending on the depth of the enamel. It has been reported that the outer surface of the enamel has smaller rods (~3 um) and wider interrod regions (~2 um).[119] On a higher level, the rods and interrods further assemble into a distinct structural pattern (Fig. 10E), which presents differing arrangements across the thickness of the enamel layer in the enamel. In a superlayer of human molar enamel, the rods are oriented radially and intercept the occlusal surface perpendicularly.[120] In the inner two-thirds of the enamel, the enamel rods deviate from the long axis in an undulating or weaving pattern, which is generally referred to as "decussation".[121]

The complex hierarchical microstructure is believed to be a key factor responsible for the unique anisotropic mechanical properties of enamel.[9, 112, 122-126] Because of the changing arrangements of the enamel rods, the hardness and elastic modulus decrease gradually from the occlusal surface of the enamel to the DEJ. Besides distinct declines in hardness and modulus upon moving away from the occlusal surface, the mechanical properties of the enamel also differ from the lingual to the buccal side of the molar.[127]

Besides the enamel structure, the chemical composition also plays an important role in determining the mechanical behavior of enamel. Xie *et al*.[128] found that an increase of protein content is the primary factor that causes the deterioration of stiffness or elastic modulus of hypomineralized enamel. Due to their higher protein content, the nanohardness and elastic modulus of the tested enamel sheaths were about 73.6 % and 52.7 % lower than those of the enamel rods, respectively.[129] The organic matter in the rod sheaths contributes significantly to the strengthening and toughening of the enamel, which is reflected by increasing crack growth resistance with crack extension from the outer to the inner enamel.[119, 123, 130] In addition, it was also suggested that the mechanical properties of enamel were also dependent on its magnesium (Mg), sodium (Na) and carbonate (CO_3^{2-}) contents.[125, 127]

3.2 Biomimetic systems for enamel reconstruction

In the last few decades, various biomimetic systems have been developed for the synthesis of biomaterials with the enamel-like structure at the nanoscale level (Table 2). Here, we review progress in the development of biomimetic systems for enamel restoration containing calcium phosphate nanoparticles, peptide, amelogenin-inspired polymers, and other organic additives. We will summarize our latest efforts to utilize amelogenin in the biomimetic reconstruction of enamel.

3.2.1 Biomimetic systems based on calcium phosphate nanoparticles

In recent years, biomimetic treatment of caries lesions by the application of calcium phosphate (CaP) materials has received considerable attention. Various types of biomimetic systems containing nanoparticles of amorphous calcium phosphate (ACP) or hydroxyapatite (HAP) have been developed for enamel regrowth.[131-138]

ACP has been proposed to be an essential precursor phase during the formation of mineralized tissue. The unique role of ACP makes it a potential remineralizing agent for the preservation and repair of tooth structures.[139,140] The effectiveness of a nanocomposite containing nanoparticles of amorphous calcium phosphate (NACP) on enamel remineralization was evaluated *in vitro*.[131] Quantitative microradiography showed that the NACP nanocomposite promoted significantly more enamel remineralization (21.8 ± 3.7%) than a fluoride-releasing composite control (5.7 ± 6.9%). This result indicated the ability of ACP nanocomposite in the remineralization of demineralized tooth structures; however, the metastable nature of ACP tremendously limits its application in clinic. ACP is more soluble than the crystalline polymorphs of calcium phosphate, so it readily converts to HAP in aqueous solution. To tackle this limitation, several systems were developed to stabilize and carry the ACP for enamel repair. For example, phosphorylated chitosan was used to stabilize ACP in a calcification solution to remineralize enamel subsurface lesions.[132] An electrospun hydrogel mat of ACP/PVP (poly(vinylpyrrolidone)) nanofibers was also developed for the *in vitro* remineralization of dental enamel.[133] The application of the ACP/PVP hydrogel mat resulted in transformation of the spherical ACP phase *in situ* at the

surface of the enamel to produce a contiguous overlayer of crystalline fluoridated hydroxyapatite with a approximately 500 nm thickness. While the lesions were remineralized, no enamel-like structure formed on the remineralized enamel surface. Instead, the surface was textured with filament-like structures approximately 1 μm in length, along with small spherical particles around 250 nm in diameter (Fig. 11A). These *in vitro* studies demonstrate the potential of ACP-based materials in the repair and prevention of initial enamel lesions; however, these effects have not yet been confirmed in a clinical trial.

Beside ACP, synthetic apatite is also considered as a promising agent for biomimetic regrowth of human enamel because of the chemical similarity to tooth enamel. Yamagishi *et al.* [134, 135] have prepared a white crystalline paste of modified hydroxyapatite (HAP), which chemically and structurally resembles natural enamel, and used it to repair an early caries lesion in a lower premolar tooth.[134,135] The artificially formed enamel-like layer was about 10 μm thick and was formed seamlessly on the enamel within 15 minutes. Unfortunately, the paste is highly acidic (pH 3.5) and contains high concentrations of hydrogen peroxide. In another biomimetic approach, nano-sized HAP particles were used to repair initial submicrometer enamel erosions.[136] It was suggested that repair at the enamel surface could be greatly improved if the size of the apatite particles are adapted to the scale of the nano-defects caused by erosive demineralization of the natural apatite crystallites. *In vitro* experimental results revealed that the HAP with a size of 20 nm adsorbed strongly to the enamel surface and further reinforced the acid-etched enamel. In contrast, these outcomes have not been observed when the large-sized HAP (> 100 nm) and ACP are applied to the erosive enamel surface. Interestingly, a repaired layer with enamel-like structure was formed under physiological conditions when glumatic acid (Glu) was introduced in this system (Fig. 11B).[137] It was proposed that the nano-apatite particles absorbed onto the enamel substrate were the building blocks, while the Glu selectively adsorbed onto the apatite (001) faces and induced oriented aggregation using the end carboxylate groups.

3.2.2 Biomimetic systems based on peptides

Inspired by the functions of proteins in tooth formation, various peptides have been synthesized to repair enamel defects. For instant, an anionic peptide (P_{11}-4, Ace-Gln-Gln-Arg-Phe-Glu-Trp-Glu-Phe-Glu-Gln-Gln-NH_2) was synthesized and shown a potential to introduce apatite mineralization to caries-like lesions in human dental enamel.[141] Recently, Li *et al.*[142] fabricated an anionic oligopeptide amphiphile (OPA, $C_{18}H_{35}O$-Thr-Lys-Arg-Glu-Glu-Val-Asp) that contains the hydrophilic functional domain of amelogenin to initialize hydroxyapatite nucleation and promote biomimetic mineralization of demineralized enamel. It was shown that apatite crystals were formed on the etched enamel after treated with OPA peptide.

Some other researchers have focused on biomimetic approaches for enamel remineralization based on the peptide derived from dentin phosphoprotein (DPP),[141, 143-148] which is the most abundant non-collagenous extracellular matrix protein in dentin. Human DPP contains numerous repetitive nucleotide sequences of aspartate-serine-serine (DSS) that are believed to promote the formation of hydroxyapatite. Several small peptides consisting of multiple repeats of the tripeptide DSS have been designed based on the DPP sequence.[143] Of the multiple-DSS peptides tested so far, a peptide carrying 8 repeats (8DSS) has been shown to promote mineral deposition onto human enamel and improve the surface properties of demineralized enamel in *in vitro* studies.[144] Mineral loss after 12 days of pH cycling was significantly lower in samples treated with 8DSS than in the control buffer-only samples, and lesions in the 8DSS samples were significantly less deep. In another study, samples treated with 8DSS had significantly higher mineral content than buffer-only samples in the region extending from the surface layer (30 μm) to the average lesion depth (110 μm).[145] Moreover, high-magnification SEM revealed a definitive change in surface morphology, from elongated hydroxyapatite nanorods in the demineralized enamel to nanoscale flakes.[144] (Fig. 11C)

3.2.3 Biomimetic systems based on amelogenin-inspired dendrimers

Poly(amido amine) (PAMAM) dendrimers have been used as "artificial proteins" and investigated as a biomineralized material, especially in the crystallization process of HAP. It has

been reported that PAMAM-type dentrimers or dendrons have a self-assembly behavior similar to that of amelogenin. For example, an amphiphilic PAMAM dendron was observed to initially self-assemble into nanospheres and further translated to linear chains in aqueous solution.[149] In another study, Yang *et al.* [150] demonstrated that carboxyl terminated PAMAM dendrimers had a strong tendency to self-assemble into hierarchical structures with the morphology of nanospheres, subsequent nanochains and microfibers, and finally macroscopic aggregates consisting of microribbons, which is similar to that of amelogenin. Furthermore, these dendrimer assemblies exhibited a function similar to amelogenin in controlling the oriented growth of HAP.[149] It was found that the apatite crystals formed in the presence of the linear assemblies resembled some of the features of the lowest level of the hierarchical structure of enamel, such as the preferential orientation of the c-axis of the HAP crystals along the amelogenin aggregates (Fig. 10).

Accordingly, several PAMAM-based dendrimers have been synthesized as the amelogenin analogs on the remineralization process of acid-etched human tooth enamel.[151-153] Wu *et al.*[152] shown that alendronate-conjugated PAMAM dendrimer (ALN-PAMAM-COOH) could induce *in situ* remineralization of tooth enamel, attributed to the combined effect of the HA-anchored property of the ALN moiety and the remineralization capability of the –COOH moiety. In addition, the newly formed crystals had nanorod-like structure similar to that of human tooth enamel (Fig. 11D). Most recently, a phosphate-terminated dendrimer (PAMAM-PO_3H_2) was synthesized and assessed for the ability to remineralize acid-etched human tooth enamel.[153] After being incubated in artificial saliva for 3 weeks, a newly generated HAP layer of 11.23 μm thickness was found on acid-etched tooth enamel treated with PAMAM-PO_3H_2.

3.2.4 Amelogenin-containing hydrogels for human enamel regrowth

A very promising route to achieve oriented enamel-like materials would be the *in situ* remineralization of enamel in the presence of amelogenin and other enamel matrix proteins.[8] We have used several strategies to prepare enamel-like materials that contain nano- and

microstructures using amelogenin to control the crystallization of biomimetic calcium and phosphate.[8, 79, 154-157] For example, using an electrolytic deposition (ELD) technique, we have synthesized an enamel-mimicking composite coating from a mineralization solution containing soluble recombinant amelogenin proteins at near-physiological pH and ionic strength.[154] A modified biomimetic approach in the presence of mineralization-modulating amelogenin was implemented to rebuild enamel structure on an acid-etched enamel surface as a model for demineralized enamel.[155] In another study, an amelogenin-releasing agar hydrogel containing calcium, phosphate, and fluoride was prepared to remineralize etched enamel in a cyclic treatment model and multispecies oral biofilm model.[156] Repetitive application of this hydrogel significantly improved enamel hardness continuously over time. These results have opened up the promising possibility of remodeling complex enamel minerals in an amelogenin-containing system.

Most recently, taking advantage of the potential of amelogenin to control the organized growth of apatite crystals and the potential antimicrobial activity of chitosan, we have developed a new amelogenin-containing chitosan (CS-AMEL) hydrogel for superficial enamel reconstruction.[158-160] It was suggested that amelogenin assemblies carried in chitosan hydrogel could stabilize Ca-P clusters and arrange them into linear chains, which fuse with enamel crystals and then develop into enamel-like co-aligned crystals.[158] After treatment with CS-AMEL hydrogel for 7 days, an enamel-like layer with a thickness of 15 μm was formed on an etched enamel surface. The newly grown layer was made of highly ordered arrays of crystals with a diameter of ~50 nm, growing preferentially along the c-axis, perpendicular to the surface. (Fig. 12A) It is noteworthy that these needle-like crystals were organized into bundles, which are similar to the fundamental units of natural enamel within the prisms. The organized enamel-like layer formed in the CS-AMEL hydrogel significantly improved the hardness and elastic modulus of the etched enamel.[158] Importantly, this biomimetic *in situ* regrowth of apatite crystals generated a robust enamel-restoration interface, which is important for ensuring the efficacy and durability of restorations

(Fig. 12B-C).[158] In a follow-up study, we optimized the conditions to produce organized enamel-like crystals in a CS-AMEL hydrogel (Fig. 12D). [159]

Compared with other biomimetic treatments, CS-AMEL hydrogel is easier to prepare for clinical use. Besides its biocompatibility and biodegradability, it has unique antimicrobial and adhesion properties that are important for dental applications. Another advantage is that the robust interface between the synthetic and natural enamel crystals promotes strong bonding between the newly grown layer and the tooth surface.

However the CS-AMEL technology still has the following limitations: (i) the hardness and modulus still do not meet the level of natural healthy enamel due to the presence of organic material and lack of hierarchical prismatic-interprismatic structure; and (ii) the extended amount of time (3-7 days) needed for the hydrogel to dry and mineralization to complete could be a challenge in a clinical setting.[160] Further studies are needed to overcome these limitations. One possible strategy to improve the mechanical properties will be the repeated application of CS-AMEL hydrogel to obtain a thicker repaired layer. Digestion of the organic material during the mineralization process is another strategy for improving the mechanical properties. In addition, to test biomimetic approaches like this one properly, it is necessary to develop a caries model system that accounts for the effects of salivary proteins on crystal growth.

Beside the full-length amelogenin, the leucine-rich amelogenin peptide (LRAP) is another candidate for biomimetic approaches for enamel reconstruction. LRAP is a 59-residue splice variant of amelogenin and contains the N- and C-terminal charged regions of the full-length amelogenin. In vitro studies have shown that LRAP has striking similarities with full-length amelogenin in respects of assembly and protein-mineral interaction.[66, 161] Furthermore, LRAP could stabilize ACP and guide ACP transformation into ordered bundles of apatite crystals.[161] Base on these evidences, it is reasonable to propose that LRAP, like full-length amelogenin, also has a great potential for biomimetic regrowth of tooth enamel.

3.2.5 Other biomimetic systems

Other biomimetic systems have been developed to repair enamel defects, including liquids and hydrogels that contain different organic additives.[162-166] A glycerine-enriched gelatin system has been used to form dense fluorapatite layers on human enamel.[162, 163] Reconstructed layers containing ordered enamel-like structures of fluoride-substituted hydroxyapatite microcrystals were synthesized on a human enamel surface using ethylenediaminetetraacetic acid disodium salt dehydrate (EDTA) as the mediating agent under near-physiological conditions.[164, 165] It was also reported that a regrown layer with prism-like hydroxyapatite can be formed on an enamel surface by an agarose hydrogel in the presence of calcium ions and a high concentration of fluoride (Fig. 13).[166]

4 Concluding remarks and future challenges

Enormous progress has been made over the last few decades in identification of the gene products involved in dental enamel formation and elucidation of their function. With advances in nanoscience and molecular biology, we now have acquired more knowledge about the unique characteristic of amelogenin and its specific interaction with different targets such as mineral, non-amelogenin proteins, cell surfaces, and proteinases.

We learned that the extended and flexible structure of amelogenin may provide the structural adaptability that facilitates the assembly of amelogenin into different quaternary structures as well as facilitates interaction with various potential targets in the enamel extracellular matrix. Amelogenin may be functional *in vivo* in oligomeric, dimeric, or even monomeric forms depending on the surface that amelogenin interacts with. A clear model for *in vivo* functional units of amelogenin however is still lacking. Amelogenin molecules do not occur in isolation *in vivo*, so the presence of other components such as mineral, other proteins, cell surface and lipid particles needs to be considered. While apatite nucleation is promoted by amelogenin *in vitro,* there is no direct evidence that enamel mineralization occurs *in vivo* via amelogenin-mediated heterogeneous nucleation. This is because enamel mineralization still occurs in amelogenin null mice and this observation does not support a direct nucleating function for amelogenin *in vivo*. A

classical theory of enamel biomineralization in which the organic matrix controls the shape of crystallites by specifically inhibiting ion deposition on the crystal sides, and orient them by binding multiple crystallites is supported by many *in vitro* studies. However, observations from loss of function studies using knock- out animal models do not support such mechanisms. The non-classical mineralization pathway which involves co-assembly of the organic matrix and the inorganic transient phase to result in elongated crystals may well explain enamel mineral formation at the early stage, but growth of the final ribbon-shaped morphology of enamel crystals cannot be easily explained by the non-classical mineralization pathway. In the maturation stage the apatite crystals mainly grow in thickness and width with concomitant and dynamic processing of the enamel matrix, and the non-classical theory cannot explain this.

In summary, understanding of the detailed underlying mechanisms of enamel formation is far from complete. In particular, extended *in vitro* and *in vivo* studies are still needed to achieve a deeper understanding of how amelogenin, associated with the non-amelogenin protein components, interact with each other and with the ameloblast cell surface as well as mineral phase, and finally produce a highly mineralized and hierarchically structured biological material.

Understanding mechanisms of protein-mediated enamel biomineralization provides a valuable foundation for development of biomaterials with composition and structures similar to enamel. In the last decade, various biomimetic systems have been investigated to mimic the enamel-like microstructures in the presence of calcium phosphate nanoparticles, peptides, amelogenin-inspired polymers, and other organic additives. Despite all these promising studies, the biomimetic strategies still face ongoing challenges in the fields of dentistry and material sciences. To date, a material that can completely take the place of human dental enamel with similar biological and mechanical properties has not yet been fabricated. Human teeth have a more complicated structure, better mechanical properties and better biocompatibility than any enamel-mimic material mentioned in this review. All the existing biomimetic materials are limited to

mimicking the enamel structure on the nanoscale level. Fabrication of the complex hierarchical rod-and-interrod structures of enamel is still a major challenge for the materials scientists of today.

Additional studies are required to evaluate the clinical applicability of the biomimetic materials mentioned. The clinical application of the existing biomimetic approaches for the treatment of larger visible cavities in the enamel is not yet conceivable. The growth of a repaired enamel layer usually takes an extended amount of time (from several hours to days, sometimes even few weeks) in the classical biomimetic strategies, which will dramatically limit the application of these materials in the clinical setting.

The CS-AMEL hydrogel we recently developed has shown a great potential for biomimetic reconstruction of enamel because of its antimicrobial property and the robust interface between the synthetic and natural enamel crystals. However the amelogenin-containing system still does not fully replicated the entire process to produce materials identical to natural enamel. While it has been established that the non- amelogenin proteins (enamelin, ameloblastin, proteinases) are also critical for controlling enamel mineralization, their application in the development of biomimetic systems remains to be explored.

Acknowledgements: Research was supported by NIH-NIDCR R01 grants; DE-13414 and DE 020099, and the USC Coulter Translational Program.

5 Reference

1. F. Nudelman and N. Sommerdijk, *Angew. Chem.Int. Edit.*, 2012, **51**, 6582-6596.
2. L. C. Palmer, C. J. Newcomb, S. R. Kaltz, E. D. Spoerke and S. I. Stupp, *Chem. Rev.*, 2008, **108**, 4754-4783.
3. N. Sommerdijk and H. Colfen, *MRS Bull.*, 2010, **35**, 116-121.
4. J. Moradian-Oldak and Y. Fan, in *Nanomaterials for the life sciences: Biomimetic and bioinspired nanomaterials*, ed. C. Kumar, Willey-VCH, Weinheim, 2010, ch. 2, pp. 41-88.
5. S. Mann, in *Dental Enamel*, John Wiley & Sons Ltd, Chichester, 1997, pp. 261-274.

6. M. A. Meyers, P. Y. Chen, A. Y. M. Lin and Y. Seki, *Prog. Mater. Sci.*, 2008, **53**, 1-206.

7. W. Kunz and M. Kellermeier, *Science*, 2009, **323**, 344-345.

8. J. Moradian-Oldak, *Front. Biosci.*, 2012, **17**, 1996-2023.

9. Z. H. Xie, E. K. Mahoney, N. M. Kilpatrick, M. V. Swain and M. Hoffman, *Acta Biomater.*, 2007, **3**, 865-872.

10. C. Robinson, P. Fuchs, D. Deutsch and J. A. Weatherell, *Caries Res.*, 1978, **12**, 1-11.

11. C. E. Smith, *Crit. Rev. Oral Biol. Med.*, 1998, **9**, 128-161.

12. J. C. C. Hu, Y. H. P. Chun, T. Al Hazzazzi and J. P. Simmer, *Cells Tissues Organs*, 2007, **186**, 78-85.

13. J. D. Bartlett, *ISRN Dentistry*, 2013, **2013**, 24.

14. A. G. Fincham, J. Moradian-Oldak and J. P. Simmer, *J. Struct. Biol.*, 1999, **126**, 270-299.

15. C. W. Gibson, Z. A. Yuan, B. Hall, G. Longenecker, E. H. Chen, T. Thyagarajan, T. Sreenath, J. T. Wright, S. Decker, R. Piddington, G. Harrison and A. B. Kulkarni, *J. Biol. Chem.*, 2001, **276**, 31871-31875.

16. J. T. Wright, Y. Li, C. Suggs, M. A. Kuehl, A. B. Kulkarni and C. W. Gibson, *Eur. J. Oral Sci.*, 2011, **119**, 65-69.

17. M. Iijima and J. Moradian-Oldak, *Calcified Tissue Int.*, 2004, **74**, 522-531.

18. M. Iijima and J. Moradian-Oldak, *J. Mater. Chem.*, 2004, **14**, 2189-2199.

19. E. Beniash, R. A. Metzler, R. S. K. Lam and P. Gilbert, *J. Struct. Biol.*, 2009, **166**, 133-143.

20. E. Beniash, J. P. Simmer and H. C. Margolis, *J. Struct. Biol.*, 2005, **149**, 182-190.

21. X. Yang, L. Wang, Y. Qin, Z. Sun, Z. J. Henneman, J. Moradian-Oldak and G. H. Nancollas, *J. Phys. Chem. B*, 2010, **114**, 2293-2300.

22. J. P. Simmer, P. Papagerakis, C. E. Smith, D. C. Fisher, A. N. Rountrey, L. Zheng and J. C. C. Hu, *J. Dent. Res.*, 2010, **89**, 1024-1038.

23. H. C. Margolis, S. Y. Kwak and H. Yamazaki, *Front. Physiol.*, 2014, **5**.

24. H. C. Margolis, E. Beniash and C. E. Fowler, *J. Dent. Res.*, 2006, **85**, 775-793.

25. C. Robinson, J. Kirkham and A. Fincham, *Connect. Tissue Res.*, 1989, **22**, 93-100.

26. M. Hannig and C. Hannig, *Nat. Nanotechnol.,* 2010, **5**, 565-569.

27. K. Delak, C. Harcup, R. Lakshminarayanan, Z. Sun, Y. Fan, J. Moradian-Oldak and J. S. Evans, *Biochemistry*, 2009, **48**, 2272-2281.

28. M. L. Snead, M. Zeichner-David, T. Chandra, K. J. Robson, S. L. Woo and H. C. Slavkin, *Proc. Natl. Acad. Sci. U S A*, 1983, **80**, 7254-7258.

29. A. G. Fincham, A. B. Belcourt, J. D. Termine, W. T. Butler and W. C. Cothran, *Biosci. Rep.*, 1981, **1**, 771-778.

30. J. Y. Sire, S. Delgado, D. Fromentin and M. Girondot, *Arch. Oral Biol.*, 2005, **50**, 205-212.

31. F. B. Wiedemann-Bidlack, S.-Y. Kwak, E. Beniash, Y. Yamakoshi, J. P. Simmer and H. C. Margolis, *J. Struct. Biol.*, 2011, **173**, 250-260.

32. J. Moradian-Oldak and R. Lakshminarayanan, in *Amelogenins: Multifaceted Proteins For Dental And Bone Formation*, ed. M. Goldberg, Bentham Science Publishers Ltd., Dubai, 2010, ch. 10, pp.106-132.

33. R. Lakshminarayanan, I. Yoon, B. G. Hegde, D. Fan, C. Du and J. Moradian-Oldak, *Proteins.*, 2009, **76**, 560-569.

34. P. Tompa, *Trends Biochem. Sci.*, 2002, **27**, 527-533.

35. C. T. Paine, M. L. Paine and M. L. Snead, *Connect. Tissue Res.*, 1998, **38**, 257-267.

36. J. Moradian-Oldak, M. L. Paine, Y. P. Lei, A. G. Fincham and M. L. Snead, *J. Struct. Biol.*, 2000, **131**, 27-37.

37. R. M. H. Ravindranath, J. Moradian-Oldak and A. G. Fincham, *J. Biol. Chem.*, 1999, **274**, 2464-2471.

38. M. L. Paine, S. N. White, W. Luo, H. Fong, M. Sarikaya and M. L. Snead, *Matrix Biol.*, 2001, **20**, 273-292.

39. M. L. Paine and M. L. Snead, *J. bone miner.*, 1997, **12**, 221-227.

40. M. Ndao, K. Dutta, K. M. Bromley, R. Lakshminarayanan, Z. Sun, G. Rewari, J. Moradian-Oldak and J. S. Evans, *Protein Sci.*, 2011, **20**, 724-734.

41. K. B. Chandrababu, K. Dutta, S. B. Lokappa, M. Ndao, J. S. Evans and J. Moradian-Oldak, *Biopolymers*, 2014, **101**, 525-535.

42. G. L. Mechanic, E. P. Katz and M. J. Glimcher, *Biochim. Biophys. Acta*, 1967, **133**, 97-113.

43. C. Du, G. Falini, S. Fermani, C. Abbott and J. Moradian-Oldak, *Science*, 2005, **307**, 1450-1454. [Erratum, Science 2005; 309: 2166].

44. P.-A. Fang, J. F. Conway, H. C. Margolis, J. P. Simmer and E. Beniash, *Proc. Natl. Acad. Sci. USA*, 2011, **108**, 14097-14102.

45. O. Martinez-Avila, S. Wu, S. J. Kim, Y. Cheng, F. Khan, R. Samudrala, A. Sali, J. A. Horst and S. Habelitz, *Biomacromolecules*, 2012, **13**, 3494-3502.

46. H. B. Wen, A. G. Fincham and J. Moradian-Oldak, *Matrix Biol.*, 2001, **20**, 387-395.

47. X. Yang, Z. Sun, R. Ma, D. Fan and J. Moradian-Oldak, *J Struct. Biol.*, 2011, **176**, 220-228.

48. C.-L. Chen, K. M. Bromley, J. Moradian-Oldak and J. J. DeYoreo, *J. Am. Chem. Soc.*, 2011, **133**, 17406-17413.

49. P.-A. Fang, H. C. Margolis, J. F. Conway, J. P. Simmer and E. Beniash, *J Struct. Biol.*, 2013, **183**, 250-257.

50. J. Moradian-Oldak, *Matrix Biol.*, 2001, **20**, 293-305.

51. J. Moradian-Oldak, J. P. Simmer, E. C. Lau, P. E. Sarte, H. C. Slavkin and A. G. Fincham, *Biopolymers*, 1994, **34**, 1339-1347.

52. A. G. Fincham, J. Moradian-Oldak, T. G. H. Diekwisch, D. M. Lyaruu, J. T. Wright, P. Bringas and H. C. Slavkin, *J Struct. Biol.*, 1995, **115**, 50-59.

53. A. G. Fincham, J. Moradian-Oldak, J. P. Simmer, P. Sarte, E. C. Lau, T. Diekwisch and H. C. Slavkin, *J Struct. Biol.*, 1994, **112**, 103-109.

54. K. M. Bromley, A. S. Kiss, S. B. Lokappa, R. Lakshminarayanan, D. Fan, M. Ndao, J. S. Evans and J. Moradian-Oldak, *J. Biological. Chem.*, 2011, **286**, 34643-34653.

55. J. X. Lu, Y. S. Xu, G. W. Buchko and W. J. Shaw, *J. Dent. Res.*, 2013, **92**, 1000-1004.

56. T. Diekwisch, S. David, P. Bringas, Jr., V. Santos and H. C. Slavkin, *Development*, 1993, **117**, 471-482.

57. W. Li, Y. Liu, T. Perez, J. D. Gunton, C. M. Sorensen and A. Chakrabarti, *Biophys. J.*, 2011, **101**, 2502-2506.

58. X. He, S. Wu, O. Martinez-Avila, Y. Cheng and S. Habelitz, *J. Struct. Biol.*, 2011, **174**, 203-212.

59. B. J. Tarasevich, S. Lea, W. Bernt, M. H. Engelhard and W. J. Shaw, *Biopolymers*, 2009, **91**, 103-107.

60. O. M. Martinez-Avila, S. Wu, Y. Cheng, R. Lee, F. Khan and S. Habelitz, *Eur. J. Oral Sci.*, 2011, **119**, 75-82.

61. N. Bouropoulos and J. Moradian-Oldak, *Calcif. Tissue Int.*, 2003, **72**, 599-603.

62. T. Aoba, E. C. Moreno, M. Kresak and T. Tanabe, *J. Dent. Res.*, 1989, **68**, 1331-1336.

63. Y. Doi, E. D. Eanes, H. Shimokawa and J. D. Termine, *J. Dent Res.*, 1984, **63**, 98-105.

64. J. Moradian-Oldak, I. Jimenez, D. Maltby and A. G. Fincham, *Biopolymers*, 2001, **58**, 606-616.

65. Z. Sun, D. Fan, Y. Fan, C. Du and J. Moradian-Oldak, *J. Dent. Res.*, 2008, **87**, 1133-1137.

66. W. J. Shaw, A. A. Campbell, M. L. Paine and M. L. Snead, *J Biol. Chem.*, 2004, **279**, 40263-40266.

67. W. J. Shaw, K. Ferris, B. Tarasevich and J. L. Larson, *Biophys. J.*, 2008, **94**, 3247-3257.

68. R. W. Friddle, K. Battle, V. Trubetskoy, J. Tao, E. A. Salter, J. Moradian-Oldak, J. J. De Yoreo and A. Wierzbicki, *Angew. Chem. Int. Edit.*, 2011, **50**, 7541-7545.

69. Z. Sun, W. Carpiaux, D. Fan, Y. Fan, R. Lakshminarayanan and J. Moradian-Oldak, *J. Dent. Res.*, 2010, **89**, 344-348.

70. D. L. Masica, J. J. Gray and W. J. Shaw, *J. Phys. Chem. C*, 2011, **115**, 13775-13785.

71. J. X. Lu, Y. S. Xu and W. J. Shaw, *Biochemistry*, 2013, **52**, 2196-2205.

72. J. Lu, S. D. Burton, Y. S. Xu, G. W. Buchko and W. J. Shaw, *Front. Physiol.*, 2014, **5**. Doi: 10.3389/fphys.2014.00254.

73. E. Beniash, J. P. Simmer and H. C. Margolis, *J. Dent. Res.*, 2012, **91**, 967-972.

74. B. J. Tarasevich, C. J. Howard, J. L. Larson, M. L. Snead, J. P. Simmer, M. Paine and W. J. Shaw, *J. Cryst. Growth*, 2007, **304**, 407-415.

75. V. Uskokovic, W. Li and S. Habelitz, *J. Cryst. Growth*, 2011, **316**, 106-117.

76. L. Wang, X. Guan, C. Du, J. Moradian-Oldak and G. H. Nancollas, *J. Phys. Chem. C*, 2007, **111**, 6398-6404.

77. M. Iijima, C. Du, C. Abbott, Y. Doi and J. Moradian-Oldak, *Eur. J. Oral Sci.*, 2006, **114**, 304-307.

78. M. Iijima, M. Hashimoto, N. Kohda, S. Nakagaki, T. Muguruma, K. Endo and I. Mizoguchi, *Dent. Mater. J.*, 2013, **32**, 775-780.

79. M. Iijima and J. Moradian-Oldak, *Biomaterials*, 2005, **26**, 1595-1603.

80. M. Iijima, Y. Moriwaki, T. Takagi and J. Moradian-Oldak, *J. Cryst. Growth*, 2001, **222**, 615-626.

81. M. Iijima, Y. Moriwaki, H. B. Wen, A. G. Fincham and J. Moradian-Oldak, *J. Dent. Res.*, 2002, **81**, 69-73.

82. H. B. Wen, J. Moradian-Oldak and A. G. Fincham, *J. Dent. Res.*, 2000, **79**, 1902-1906.

83. J. P. Simmer, A. S. Richardson, Y. Y. Hu, C. E. Smith and J. C. C. Hu, *Int. J. Oral Sci.*, 2012, **4**, 129-134.

84. P. Bodier-Houlle, P. Steuer, J. M. Meyer, L. Bigeard and F. J. Cuisinier, *Cell Tissue Res.*, 2000, **301**, 389-395.

85. F. J. Cuisinier, P. Steuer, B. Senger, J. C. Voegel and R. M. Frank, *Cell Tissue Res.*, 1993, **273**, 175-182.

86. T. G. Diekwisch, *Connect. Tissue Res.*, 1998, **38**, 101-111.

87. H. Masuya, K. Shimizu, H. Sezutsu, Y. Sakuraba, J. Nagano, A. Shimizu, N. Fujimoto, A. Kawai, I. Miura, H. Kaneda, K. Kobayashi, J. Ishijima, T. Maeda, Y. Gondo, T. Noda, S. Wakana and T. Shiroishi, *Hum. Mol. Genet.*, 2005, **14**, 575-583.

88. M. H. Rajpar, K. Harley, C. Laing, R. M. Davies and M. J. Dixon, *Hum. Mol. Genet.*, 2001, **10**, 1673-1677.

89. J. C. Hu, Y. Hu, C. E. Smith, M. D. McKee, J. T. Wright, Y. Yamakoshi, P. Papagerakis, G. K. Hunter, J. Q. Feng, F. Yamakoshi and J. P. Simmer, *J. Biol. Chem.*, 2008, **283**, 10858-10871.

90. J. C. Hu, Y. Hu, Y. Lu, C. E. Smith, R. Lertlam, J. T. Wright, C. Suggs, M. D. McKee, E. Beniash, M. E. Kabir and J. P. Simmer, *Plos One*, 2014, **9**, e89303.

91. Y. Yamakoshi, T. Tanabe, S. Oida, C. C. Hu, J. P. Simmer and M. Fukae, *Arch. Oral Biol.*, 2001, **46**, 1005-1014.

92. T. Tanabe, T. Aoba, E. C. Moreno, M. Fukae and M. Shimuzu, *Calcif. Tissue Int.*, 1990, **46**, 205-215.

93. N. Bouropoulos and J. Moradian-Oldak, *J. Dent. Res.*, 2004, **83**, 278-282.

94. M. Iijima, D. Fan, K. M. Bromley, Z. Sun and J. Moradian-Oldak, *Cryst. Growth Des.*, 2010, **10**, 4815-4822.

95. D. M. Fan, M. Iijima, K. M. Bromley, X. D. Yang, S. Mathew and J. Moradian-Oldak, *Cells Tissues Organs*, 2011, **194**, 194-198.

96. D. Fan, C. Du, Z. Sun, R. Lakshminarayanan and J. Moradian-Oldak, *J. Struct. Biol.*, 2009, **166**, 88-94.

97. X. Yang, D. Fan, S. Mattew and J. Moradian-Oldak, *Eur. J. Oral Sci.*, 2012, **119**, 351-356.

98. V. Gallon, L. Chen, X. Yang and J. Moradian-Oldak, *J. Struct. Biol.*, 2013, **183**, 239-249.

99. S. Fukumoto, T. Kiba, B. Hall, N. Iehara, T. Nakamura, G. Longenecker, P. H. Krebsbach, A. Nanci, A. B. Kulkarni and Y. Yamada, *J. Cell Biol.*, 2004, **167**, 973-983.

100. R. M. Wazen, P. Moffatt, S. F. Zalzal, Y. Yamada and A. Nanci, *Matrix Biol.*, 2009, **28**, 292-303.

101. S. F. Zalzal, C. E. Smith and A. Nanci, *Matrix Biol.*, 2008, **27**, 352-359.

102. J. Hatakeyama, S. Fukumoto, T. Nakamura, N. Haruyama, S. Suzuki, Y. Hatakeyama, L. Shum, C. W. Gibson, Y. Yamada and A. B. Kulkarni, *J. Dent. Res.*, 2009, **88**, 318-322.

103. M. Fukae and T. Tanabe, *Calcif. Tissue Int.*, 1987, **40**, 286-293.

104. K. Kawasaki and K. M. Weiss, *Proc. Natl. Acad. Sci. U S A*, 2003, **100**, 4060-4065.

105. C. Murakami, N. Dohi, M. Fukae, T. Tanabe, Y. Yamakoshi, K. Wakida, T. Satoda, O. Takahashi, M. Shimizu, O. H. Ryu, J. P. Simmer and T. Uchida, *Histochem. Cell Biol.*, 1997, **107**, 485-494.

106. H. H. Ravindranath, L. S. Chen, M. Zeichner-David, R. Ishima and R. M. Ravindranath, *Biochem. Biophys. Res. Commun.*, 2004, **323**, 1075-1083.

107. P. Mazumder, S. Prajapati, S. B. Lokappa, V. Gallon and J. Moradian-Oldak, *Front. Physiol.*, 2014, **5**, 274. doi: 10.3389/fphys.2014.00274.

108. D. Deutsch, J. Catalano-Sherman, L. Dafni, S. David and A. Palmon, *Connect. Tissue Res.*, 1995, **32**, 97-107.

109. S. Bekshe Lokappa, K. Balakrishna Chandrababu, K. Dutta, I. Perovic, J. Spencer Evans and J. Moradian-Oldak, *Biopolymers*, 2015, **103**, 96-108.

110. S.-Y. Kwak, S. Green, F. B. Wiedemann-Bidlack, E. Beniash, Y. Yamakoshi, J. P. Simmer and H. C. Margolis, *Eur. J. Oral Sci.*, 2011, **119**, 103-111.

111. K. M. Bromley, R. Lakshminarayanan, M. Thompson, S. B. Lokappa, V. A. Gallon, K. R. Cho, S. R. Qiu and J. Moradian-Oldak, *Cryst. Growth Des.*, 2012, **12**, 4897-4905.

112. Y. R. Zhang, W. Du, X. D. Zhou and H. Y. Yu, *Int. J. Oral Sci.*, 2014, **6**, 61-69.

113. J. Li, X. Xie, Y. Wang, W. Yin, J. S. Antoun, M. Farella and L. Mei, *J. Dent.*, 2014, **42**, 769-777.

114. V. Yengopal and S. Mickenautsch, *Acta odontol. Scand.*, 2009, **67**, 321-332.

115. J. Moradian-Oldak, *Dimes. Dent. Hyg.*, 2009, 7(8), 12-15.

116. F. Z. Cui and J. Ge, *J. Tissue Eng. Regen. Med.*, 2007, **1**, 185-191.

117. L. M. Simmons, J. Montgomery, J. Beaumont, G. R. Davis and M. Al-Jawad, *Arch. Oral Biol.*, 2013, **58**, 1726-1734.

118. J. Xue, A. V. Zavgorodniy, B. J. Kennedy, M. V. Swain and W. Li, *J. Microsc.*, 2013, **251**, 144-153.

119. L. H. He, Z. H. Yin, L. J. van Vuuren, E. A. Carter and X.-W. Liang, *Acta Biomater.*, 2013, **9**, 6330-6337.

120. T. E. Popowics, J. M. Rensberger and S. W. Herring, *Arch.. Oral Biol.*, 2004, **49**, 595-605.

121. A. Boyde, *Bull. Group. Int. Rech. Sci. Stomatol.*, 1969, **12**, 151-207.

122. B. B. An, R. R. Wang and D. S. Zhang, *Acta Biomater.*, 2012, **8**, 3784-3793.

123. D. Bajaj and D. Arola, *Acta Biomater.*, 2009, **5**, 3045-3056.

124. H. Eimar, E. Ghadimi, B. Marelli, H. Vali, S. N. Nazhat, W. M. Amin, J. Torres, O. Ciobanu, R. F. Albuquerque and F. Tamimi, *Acta Biomater.*, 2012, **8**, 3400-3410.

125. C. Xu, R. Reed, J. P. Gorski, Y. Wang and M. P. Walker, *J. Mater. Sci.*, 2012, **47**, 8035-8043.

126. B. An, R. Wang, D. Arola and D. Zhang, *J. Mech. Behav. Biomed.l Mater.*, 2012, **9**, 63-72.

127. J. L. Cuy, A. B. Mann, K. J. Livi, M. F. Teaford and T. P. Weihs, *Arch. Oral Biol.*, 2002, **47**, 281-291.

128. Z. H. Xie, M. V. Swain, G. Swadener, P. Munroe and M. Hoffman, *J. Biomech.*, 2009, **42**, 1075-1080.

129. J. Ge, F. Z. Cui, X. M. Wang and H. L. Feng, *Biomaterials*, 2005, **26**, 3333-3339.

130. D. Bajaj and D. D. Arola, *Biomaterials*, 2009, **30**, 4037-4046.

131. M. D. Weir, L. C. Chow and H. H. K. Xu, *J. Dent. Res.*, 2012, **91**, 979-984.

132. X. Zhang, Y. Li, X. Sun, A. Kishen, X. Deng, X. Yang, H. Wang, C. Cong, Y. Wang and M. Wu, *J. Mater. Sci. Mater. Med.*, 2014, **12**, 30.

133. J. Fletcher, D. Walsh, C. E. Fowler and S. Mann, *Crystengcomm*, 2011, **13**, 3692-3697.

134. K. Yamagishi, K. Onuma, T. Suzuki, F. Okada, J. Tagami, M. Otsuki and P. Senawangse, *Nature*, 2005, **433**, 819-819.

135. K. Onuma, K. Yamagishi and A. Oyane, *J. Cryst. Growth*, 2005, **282**, 199-207.

136. L. Li, H. H. Pan, J. H. Tao, X. R. Xu, C. Y. Mao, X. H. Gu and R. K. Tang, *J. Mater. Chem.*, 2008, **18**, 4079-4084.

137. L. Li, C. Mao, J. Wang, X. Xu, H. Pan, Y. Deng, X. Gu and R. Tang, *Adv. Mater.*, 2011, **23**, 4695-4701.

138. J. Wei, J. C. Wang, W. P. Shan, X. C. Liu, J. Ma, C. S. Liu, J. Fang and S. C. Wei, *J. Mater. Sci. Mater. Med.*, 2011, **22**, 1607-1614.

139. J. Zhao, Y. Liu, W. B. Sun and H. Zhang, *Chem. Cent. J.*, 2011, **5**, 7.

140. N. J. Cochrane, F. Cai, N. L. Huq, M. F. Burrow and E. C. Reynolds, *J. Dent. Res.*, 2010, **89**, 1187-1197.

141. J. Kirkham, A. Firth, D. Vernals, N. Boden, C. Robinson, R. C. Shore, S. J. Brookes and A. Aggeli, *J. Dent. Res.*, 2007, **86**, 426-430.

142. Q. L. Li, T. Y. Ning, Y. Cao, W. B. Zhang, M. L. Mei and C. H. Chu, *BMC biotechnology*, 2014, **14**, 32.

143. D. K. Yarbrough, E. Hagerman, R. Eckert, J. He, H. Choi, N. Cao, K. Le, J. Hedger, F. Qi, M. Anderson, B. Rutherford, B. Wu, S. Tetradis and W. Shi, *Calcif. Tissue Int.*, 2010, **86**, 58-66.

144. C. C. Hsu, H. Y. Chung, J. M. Yang, W. Shi and B. Wu, *J. Dent. Res.*, 2011, **90**, 88-92.

145. Y. Yang, X. P. Lv, W. Shi, J. Y. Li, D. X. Li, X. D. Zhou and L. L. Zhang, *J. Dent. Res.*, 2014, **93**, 520-524.

146. H.-Y. Chung and C.-C. Li, *J.Mater. Res.*, 2013, **28**, 2890-2896.

147. H.-Y. Chung and K.-C. Huang, *J. Mech. Behav. Biomed. Mater.*, 2013, **28**, 213-221.

148. H.-Y. Chung and C. C. Li, *Mater. Sci. Eng. C Mater. Biol. Appl.*, 2013, **33**, 969-973.

149. S. Yang, H. He, L. Wang, X. Jia and H. Feng, *Chem. Commun.*, 2011, **47**, 10100-10102.

150. J. Yang, S. Cao, J. Li, J. Xin, X. Chen, W. Wu, F. Xu and J. Li, *Soft Matter*, 2013, **9**, 7553-7559.

151. X. Yang, H. Shuang, C. Ding and J. Li, *Polym. Chem.,* 2015, **6**, 668-680.

152. D. Wu, J. Yang, J. Li, L. Chen, B. Tang, X. Chen and W. Wu, *Biomaterials*, 2013, **34**, 5036-5047.

153. M. Chen, J. Yang, J. Li, K. Liang, L. He, Z. Lin, X. Chen and X. Ren, *Acta Biomater.*, 2014, **10**, 4437-4446.

154. Y. Fan, Z. Sun, R. Wang, C. Abbott and J. Moradian-Oldak, *Biomaterials*, 2007, **28**, 3034-3042.

155. Y. Fan, Z. Sun and J. Moradian-Oldak, *Biomaterials*, 2009, **30**, 478-483.

156. Y. Fan, Z. T. Wen, S. Liao, T. Lallier, J. L. Hagan, J. T. Twomley, J.-F. Zhang, Z. Sun and X. Xu, *J. Bioact. Compat. Pol.*, 2012, **27**, 585-603.

157. H. B. Wen, J. Moradian-Oldak and A. G. Fincham, *Biomaterials*, 1999, **20**, 1717-1725.

158. Q. Ruan, Y. Zhang, X. Yang, S. Nutt and J. Moradian-Oldak, *Acta Biomater.*, 2013, **9**, 7289-7297.

159. Q. Ruan, N. Siddiqah, X. Li, S. Nutt and J. Moradian-Oldak, *Connect. Tissue Res.*, 2014, **1**, 150-154.

160. Q. Ruan and J. Moradian-Oldak, *J Vis Exp*, 2014. doi: 10.3791/51606.

161. E. Le Norcy, S. Y. Kwak, F. B. Wiedemann-Bidlack, E. Beniash, Y. Yamakoshi, J. P. Simmer and H. C. Margolis, *J. Dent. Res.*, 2011, **90**, 1091-1097.

162. A. Guentsch, S. Busch, K. Seidler, U. Kraft, S. Nietzsche, P. M. Preshaw, J. N. Chromik, E. Glockmann, K. D. Jandt and B. W. Sigusch, *Adv. Eng. Mater.*, 2010, **12**, B571-B576.

163. S. Busch, *Angew. Chem. Int. Edit.*, 2004, **43**, 1428-1431.

164. Y. J. Yin, S. Yun, J. S. Fang and H. F. Chen, *Chem. Commun.*, 2009, 5892-5894.

165. R. Q. Xie, Z. D. Feng, S. W. Li and B. B. Xu, *Cryst. Growth Des.*, 2011, **11**, 5206-5214.

166. Y. Cao, M. L. Mei, Q.-L. Li, E. C. M. Lo and C. H. Chu, *Acs Appl. Mater. Inter.*, 2014, **6**, 410-420.

Figure Captions

Figure 1. Amelogenin structural changes induced by the presence of solvents and different targets. (A) Amelogenin monomer in acidic solution; Reproduced with permission from ref 27. (B) In 70% TFE; Reproduced with permission from ref 40. (C) In 10% SDS; Reproduced with permission from ref 41. (D) Amelogenin LRAP adsorbed on HAP mineral; Reproduced with permission from ref 70. (E) In POPG. Reproduced with permission from ref 109. Red = alpha helix; Blue = extended beta strand; white = missing residue (s); Black = PPII; Yellow = RC.

Figure 2. Circular Dichroism spectra of recombinant amelogenin rp172 in increasing concentrations of TFE. Note the change in the shape of the curve with minima at 210 and 225 nm representing alpha helix conformation in 30% TFE. Reproduced with permission from ref 40.

Figure 3. Schematic representation of amelogenin's N-terminal segment showing the protein backbone around W25 residue interacting with the SDS head groups (pink circles). The protein hydrophobic side chains buried in the aliphatic tail of the SDS micelle model (thin blue lines). Reproduced with permission from ref 41.

Figure 4. Quaternary structures formed by recombinant amelogenin assembly *in vitro* under different experimental conditions; (A) AFM tapping mode (Image width = 500 nm) of amelogenin nanospheres formed at pH 8, adsorbed on mica and fixed by Karnovsky fixative; Reproduced with permission from ref 46. (B) Amelogenin nanochains detected by TEM following slow solvent evaporation in the presence of PEG. Reproduced with permission from ref 43. (C) Amelogenin oligomers formed at pH 8 and detected in cryo-TEM, Reproduced with permission from ref 44. D) AFM tapping mode (Width = 3 μM) of amelogenin nanoribbons formed at pH 4.5, and in the presence of calcium phosphate. Reproduced with permission from ref 45.

Figure 5. Schematic presentation of oligomer formation reported by Bromely et al. Reproduced with permission from ref 54. At pH 3.5, each amelogenin carries a large positive charge, electrostatically stabilizing the monomeric form. As some histidine residues become deprotonated with increasing pH, oligomers containing an average of eight monomers are formed via N-terminal mediated intermolecular interactions, though the oligomers still retain a positive charge. At pH 8, the histidine residues would be deprotonated, allowing weak hydrophobic forces to bind the oligomers together in the form of a nanosphere.

Figure 6. The molecular structure of phosphorylated LRAP adsorbed to HAp {010} surface demonstrating folding at N- and C- termini. (A) Representative structure determined with a weight *w* of 1 kcal/mol. Opacity represents LRAP's molecular shape, cartoons represent secondary structure. Predicted distance measurements at constrained atoms for the (B) N-terminal, (C) middle, and (D) C-terminal domains. Reproduced with permission from ref 70.

Figure 7. SEM images of nanostructures contained within an elongated HAP crystal that was synthesized in the presence of amelogenin using the constant composition method. (A) An area revealing that elongated HAP crystals consist of bundles of pearl-like nanothreads. The inset EDS was recorded from the rectangle in (A), showing a Ca/P ratio of 1.50. (B) Nanoparticles (30-50

nm) are connected to each other to form the nanothreads as shown within two dotted rectangles. Reproduced with permission from ref 21.

Figure 8. Circular dichroism (CD) spectra of amelogenin in association with increasing concentrating of the 32-kDa enamelin. Inset is the TEM of amelogenin-enamelin mixture labeled with anti enamelin antibody and gold conjugated secondary antibody. Reproduced with permission from ref 97.

Figure 9. Circular dichroism (CD) spectra of recombinant ameloblastin in association with amelogenin demonstrating the conformational change of ameloblastin as the result of its interaction with amelogenin. Reproduced with permission from ref 107.

Figure 10. Hierarchical structure of dental enamel from the nanoscale to microscale levels. The ruler below the diagram demonstrates the typical scale distribution of each level. (A) High resolution transmission electron microscopy (HR-TEM) and (inset) selected area electron diffraction (SAED) images of an enamel crystal, showing the lattice structure and crystal orientation of the hydroxyapatite crystal aligned along the c-axis; (B) TEM and (C) scanning electron microscopy (SEM) images of a typical bundle of parallel enamel crystals; (D) and (E) SEM images of enamel surface, showing the typical structures of (D) enamel rods and (E) prism decussation; P: prism; IP, inter-prism; (F) Schematic image showing the basic tooth anatomy. E, enamel; D, dentin; P, pulp. Enamel samples were prepared from human third molars without any restored caries (extracted following the standard procedures for extraction at the Ostrow School of Dentistry of the University of Southern California and handled with the approval of the Institutional Review Board). SEM imaging was performed in a field emission scanning electron microscope (JEOL JSM-7001F), operating at an accelerating voltage of 10keV.TEM and SAED images were obtained on a JEOL JEM-2100 microscope using an accelerating voltage of 200keV.

Figure 11. SEM images of the surfaces of enamel treated with different biomimetic systems. (A) ACP/PVP electrospun mat; filament-like structures (red arrows) and spherical particles (yellow arrows) are shown. Reproduced with permission from ref 133. (B) HAp paste with Glu in SBF solution; the insert shows the "fish-scale" feature of enamel after the repair. Black arrows indicate the crystallographic orientations of the apatite rods in enamel and white arrows indicate the apatite orientations in the artificial layer. Reproduced with permission from ref 137. (C) 8DSS peptide. Reproduced with permission from ref 144. (D) ALN-PAMAM-COOH, The inserts are enlarged details. Reproduced with permission from ref 152.

Figure 12. Biomimetic reconstruction of human enamel with amelogenin–chitosan (CS-AMEL) hydrogel. (A) SEM images of the surfaces of enamel treated with CS-AMEL hydrogel for 7 days. (B) Cross-section SEM image of the repaired layer after remineralization in CS-AMEL hydrogel for 3 days fused to the surface of the natural enamel. The white and black arrows indicate the crystallographic orientations of the crystals in the newly grown layer and natural enamel, respectively. The dotted line shows the boundary of the natural enamel and the newly grown layer. (C) HR-TEM image of the interface between the enamel and regrown crystal, showing seamless growth of the repaired crystal on the enamel. The black arrows indicate the interface between regrown and enamel crystals. (Inset) FFT images corresponding to enamel and regrown crystals.

Reproduced with permission from ref 158. (D) Optimal conditions (red region) to produce organized enamel-like crystals in a CS-AMEL hydrogel. Data are based on tables in ref 159.

Figure 13. SEM images of the surfaces of enamel treated with agarose hydrogel in the presence of 500 ppm fluoride. Reproduced with permission from ref 166.

Table 1. Amelogenin structural changes induced by different targets

Targets/solvent	Interacting domains	Structural changes	Ref.
Amelogenin (pH 5.5)	N-terminus	----	54
TFE (70%)	N- terminus C- terminus	Alpha helix Alpha helix	40
SDS (10%)	N-terminus	Alpha helix	41
Ca, PO_4^{3-} ions (pH 4.5)	N-terminus	----	45
Apatite Mineral	N-terminus* C-terminus	Helix-turn helix Beta strand	70 55,73
Enamelin	N-terminus	----	96
Ameloblastin	N-terminus	----	107
POPG (pH 3.5)	N-terminus C- terminus	Alpha helix Alpha helix	109

Abbreviations: TFE, 2,2,2-trifluoroethanol; SDS, sodium dodecyl sulfate; POPG, 1-palmitoyl-2-oleoyl-sn-glycero-3-phosphoglycerol;
* Based on amelogenin LRAP

Table 2 Biomimetic systems used for enamel reconstruction.

Biomimetic systems		Repair time	Characteristic information of repaired layers				Ref.
			Structure of regrown crystals	Thickness (μm)	Hardness (GPa[1]/VHN[2]/KHN[3])	Modulus (GPa)	
CaP based systems	ACP/PVP hydrogel	1 hours	Random filament-like structure	0.5	--	--	133
	Fluorized-apatite paste	15 minutes	Net-like structure	20	--	75.0 ± 5.0 [1]	134, 135
	HAP Paste with Glu in SBF solution	3 days	Nanorod	0.6 - 1.0	4.7±0.2 [1]	96.9 ± 4.0 [1]	137
Peptide based systems	Anionic peptide (P_{11}-4)	5 days	---	---	---	---	141
	Anionic oligopeptideamphiphile (OPA)	20 days	Nanorods	~ 5	~175 [2]	---	142
	8DSS peptide (in SBF solution)	24 hours	Random flakes	----	2.20 [1]	64.93 [1]	144, 145
Amlogenin-inspired dendrimers	ALN-PAMAM-COOH	4 weeks	Nanorods	~ 11	~350 [3]	---	152
	PAMAM -PO_3H_2	3 weeks	Nanorods	~ 11	360 [3]	---	153
Amelogenin based systems	Amelogenin (in solution)	~16 hours	Organized bundles of nanorods	---	---	---	155
	Amelogenin-agar gel	3-5 days	Nanocrystal bundles	---	114.0 ± 69.7 [3]	---	156
	CS-AMEL hydrogel	3-7 days	Organized bundles of nanorods	~ 15	0.98 ± 0.57 [1]	31.01 ± 8.85 [1]	158
Other systems	Glycerine-enriched gelatin gel	20 days	Polygons prisms	~ 10	400 ± 100 [3]	--	163
	EDTA (in solution)	5-8 days	Hexagonal rod	1.4	347-370 [2]	---	165
	Agarose hydrogel	6 days	Hexagonal rod	3.5	3.04 ± 0.75 [1]	89.46 ±11.82 [1]	166

[1]tested by a Nanoidenter; [2]tested by a Vickers microhardness tester; [3]tested by a Knoop microhardness tester.

Abbreviations: ACP, amorphous calcium phosphate; PVP, poly(vinylpyrrolidone); SBF, simulated body fluid; P_{11}-4, Ace-Gln-Gln-Arg-Phe-Glu-Trp-Glu-Phe-Glu-Gln-Gln-NH_2; OPA, $C_{18}H_{35}O$-Thr-Lys-Arg-Glu-Glu-Val-Asp; 8DSS, 8 repeats of aspartate-serine-serine; ALN-PAMAM-COOH, carboxyl-terminated poly(amidoamine) - alendronate (ALN) conjugate; PAMAM -PO_3H_2, phosphate-terminated poly(amidoamine) dendrimer; EDTA, ethylenediaminetetraacetic acid disodium salt dehydrate; CS-AMEL, amelogenin-containing chitosan hydrogel.

Note: The hardness and modulus of a healthy enamel are measured to be around 4.0 and 90 GPa under the nanoindentation tests, respectively;[128] The Vickers microhardness of healthy enamel is 276 -360 VHN.[142,164] The Knoop microhardness of healthy enamel is 372-400 KHN.[153,162]

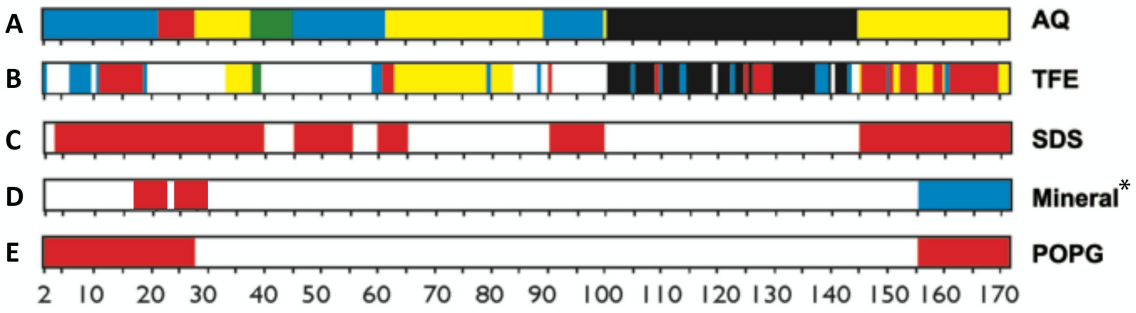

FIG 1

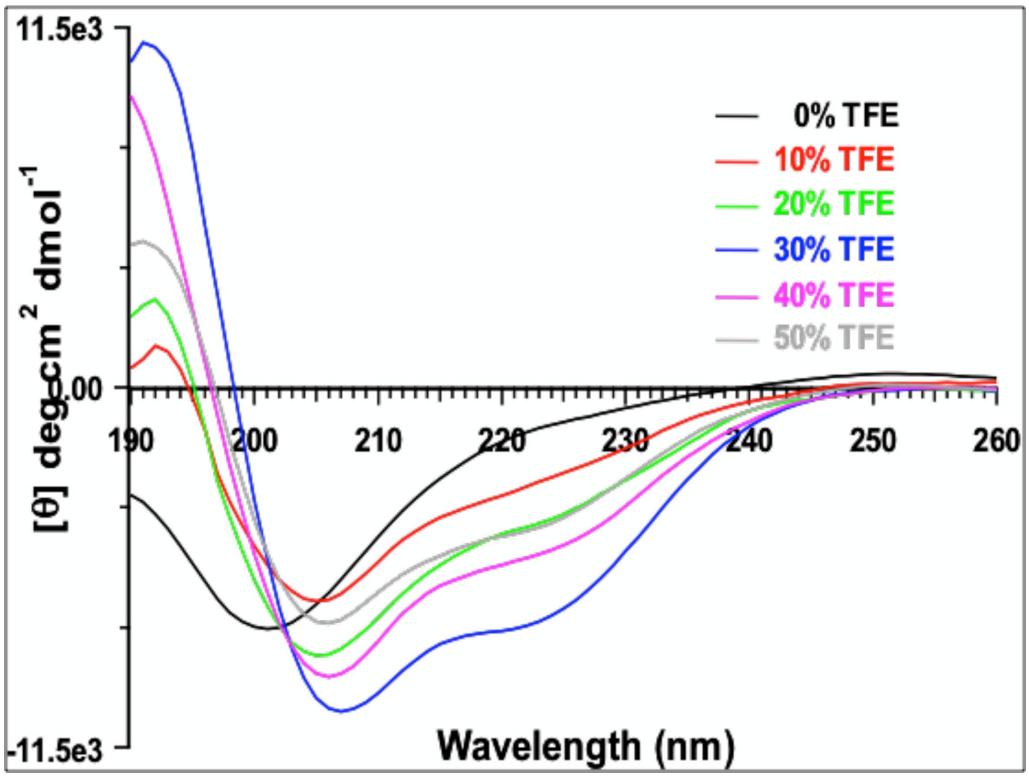

FIG 2

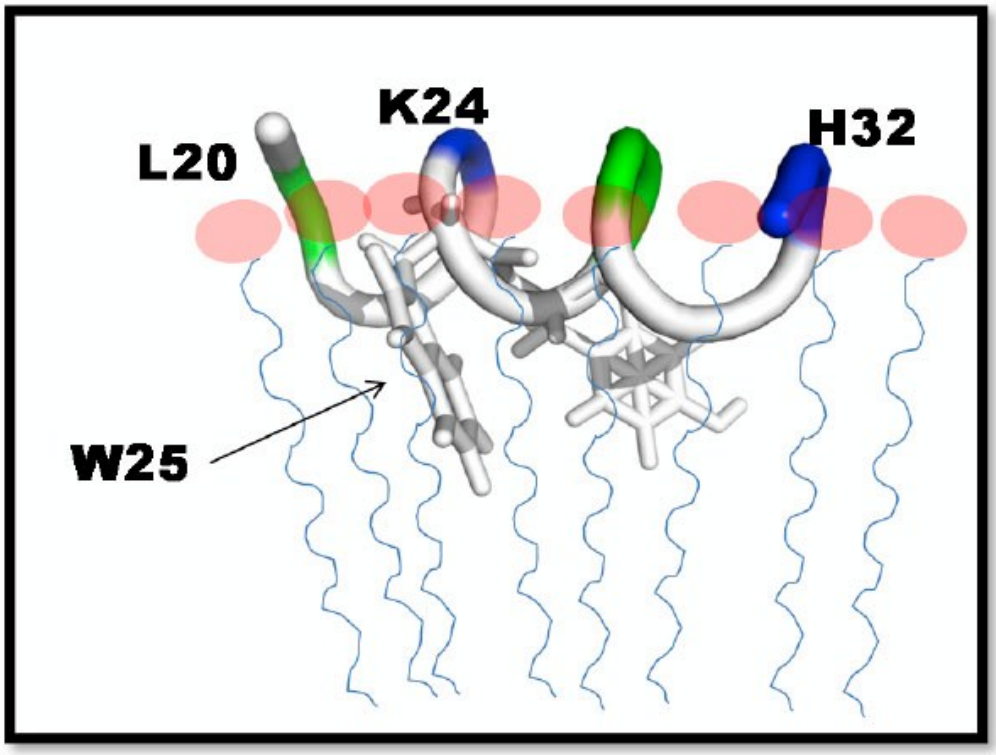

FIG 3

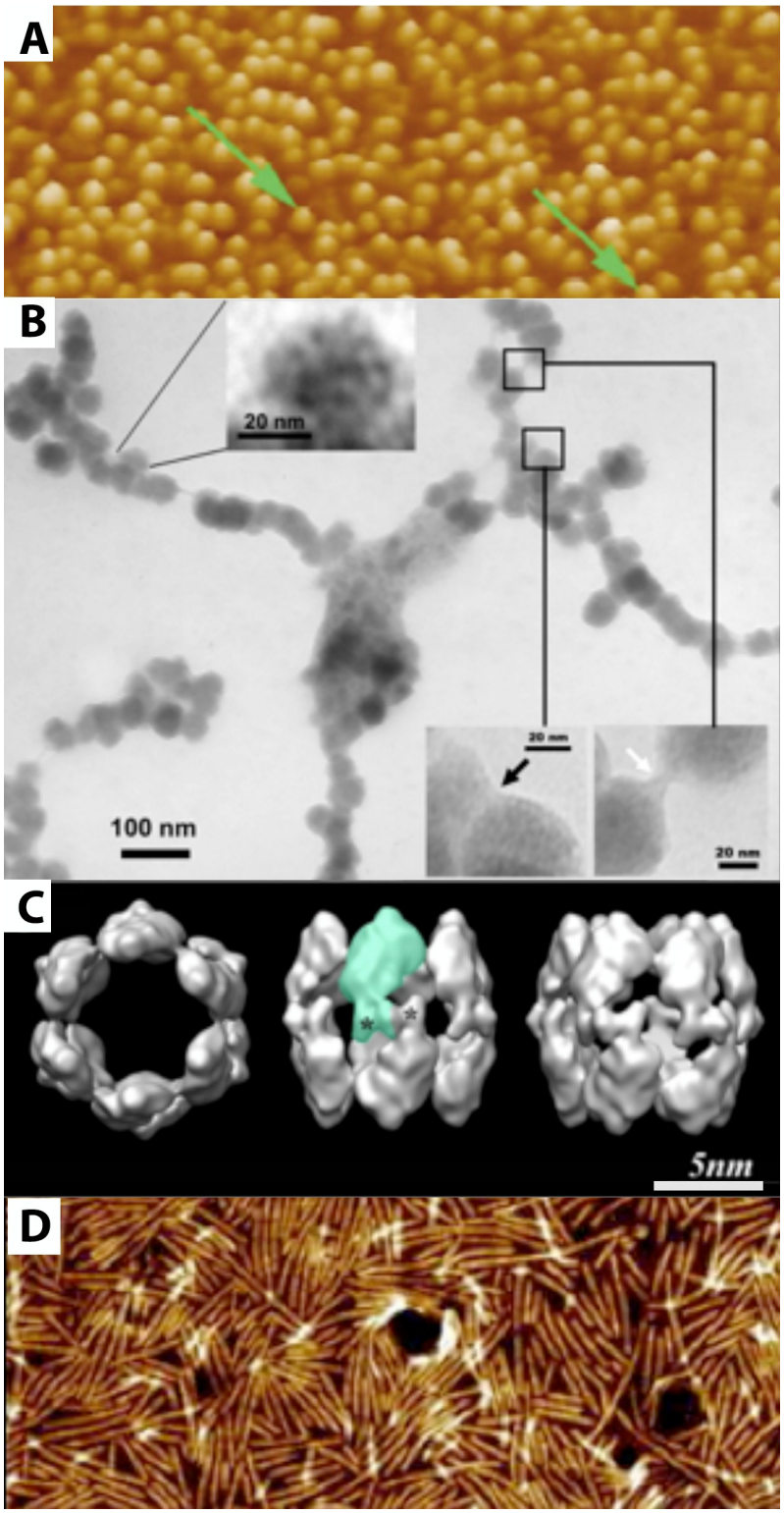

FIG 4

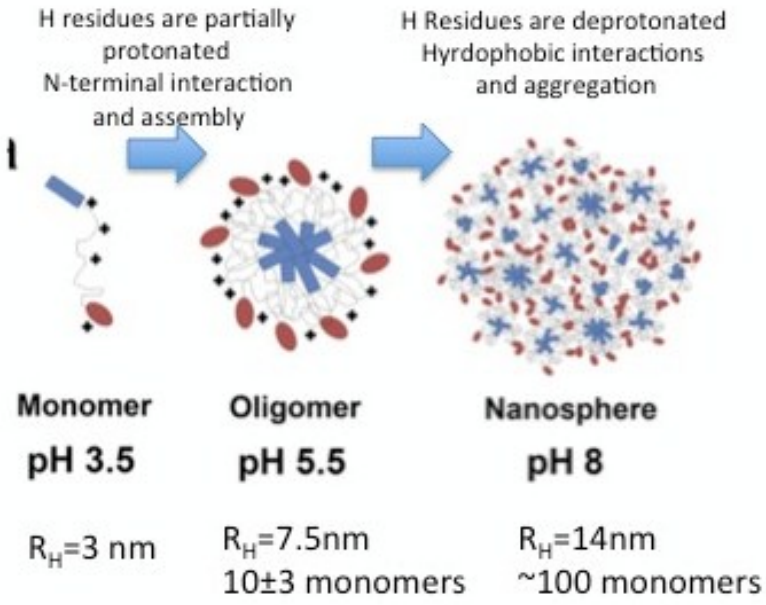

FIG 5

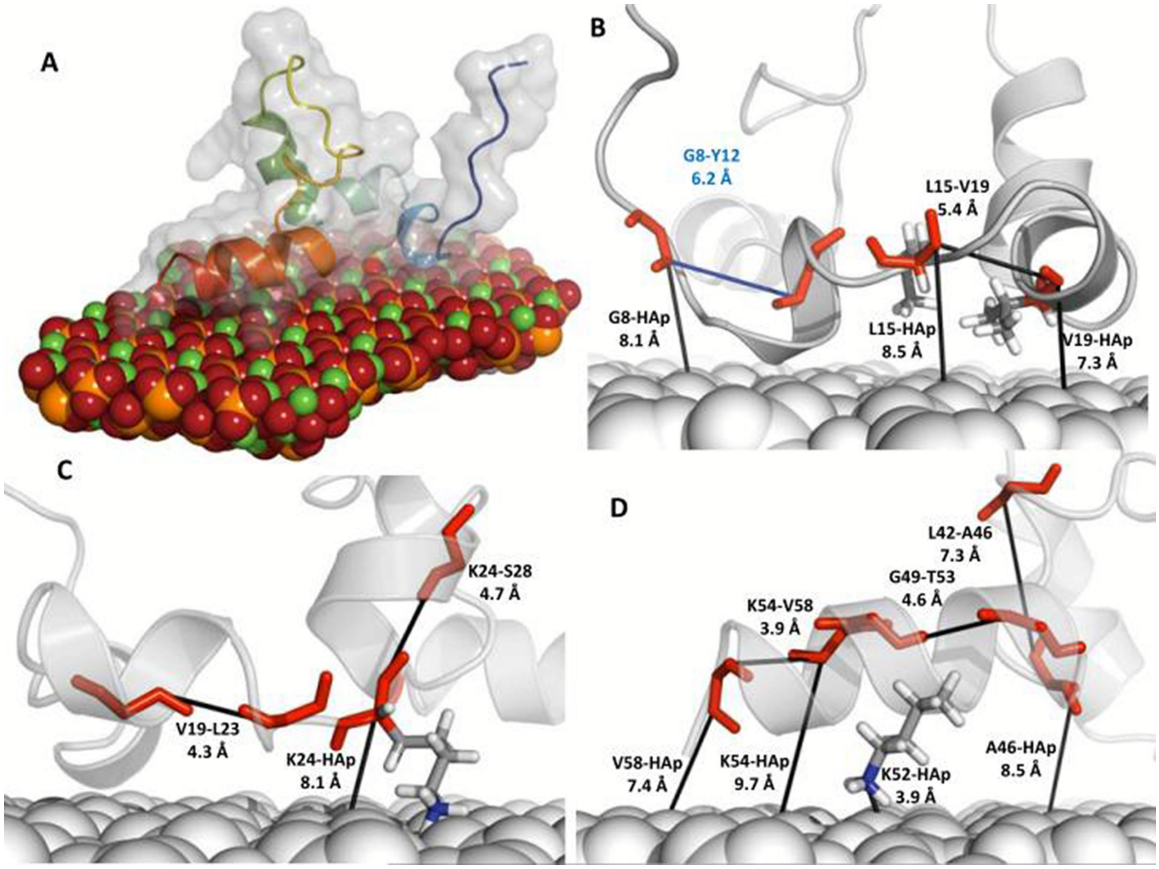

FIG 6

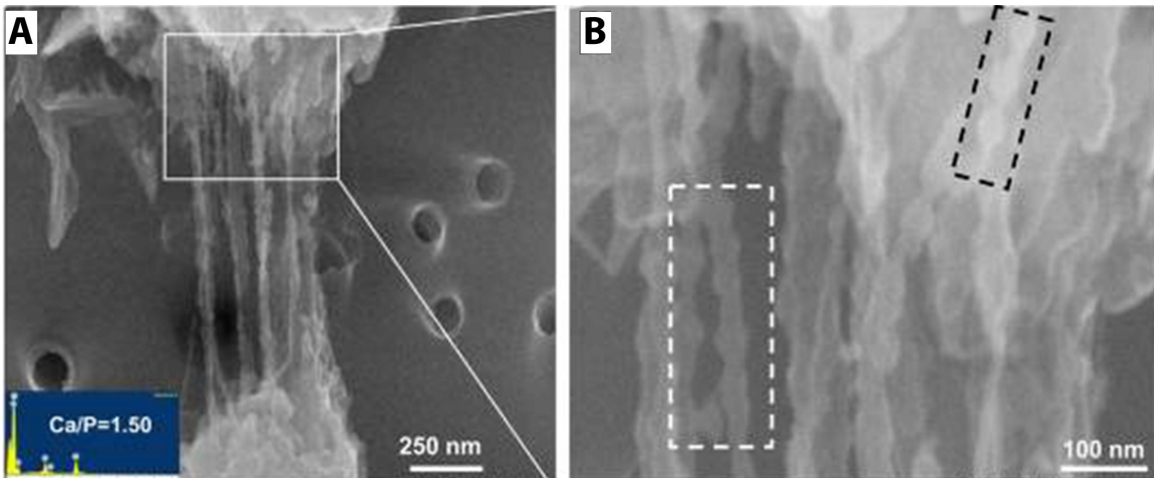

FIG 7

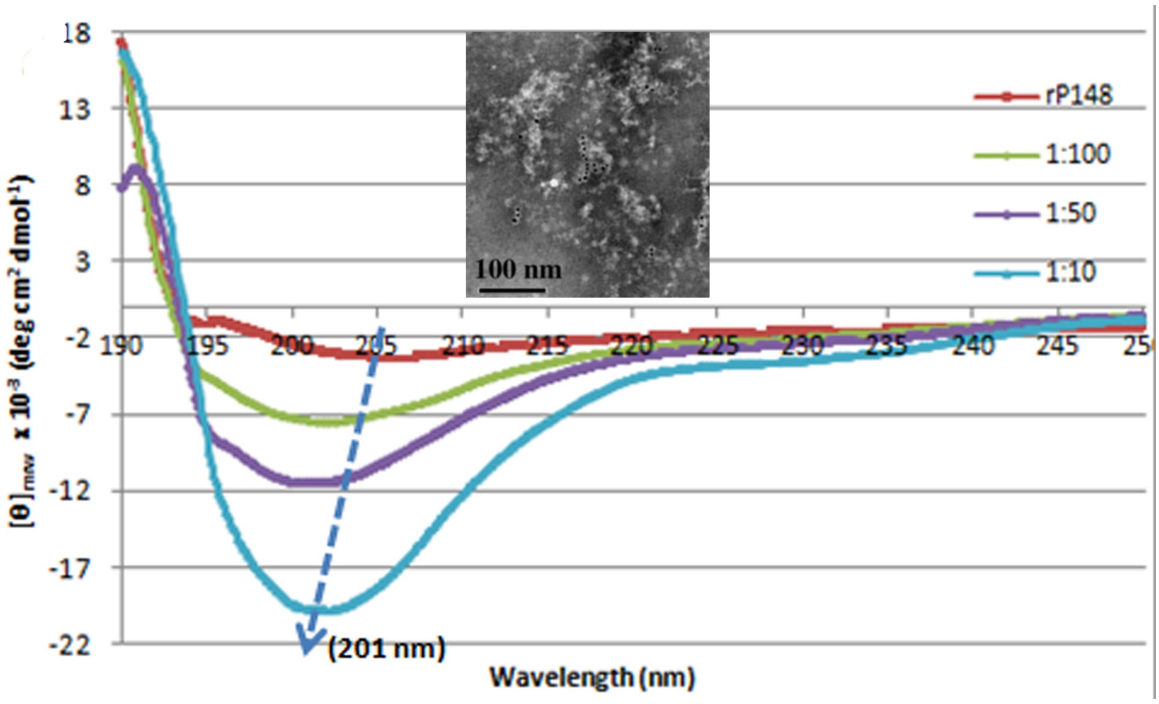

FIG 8

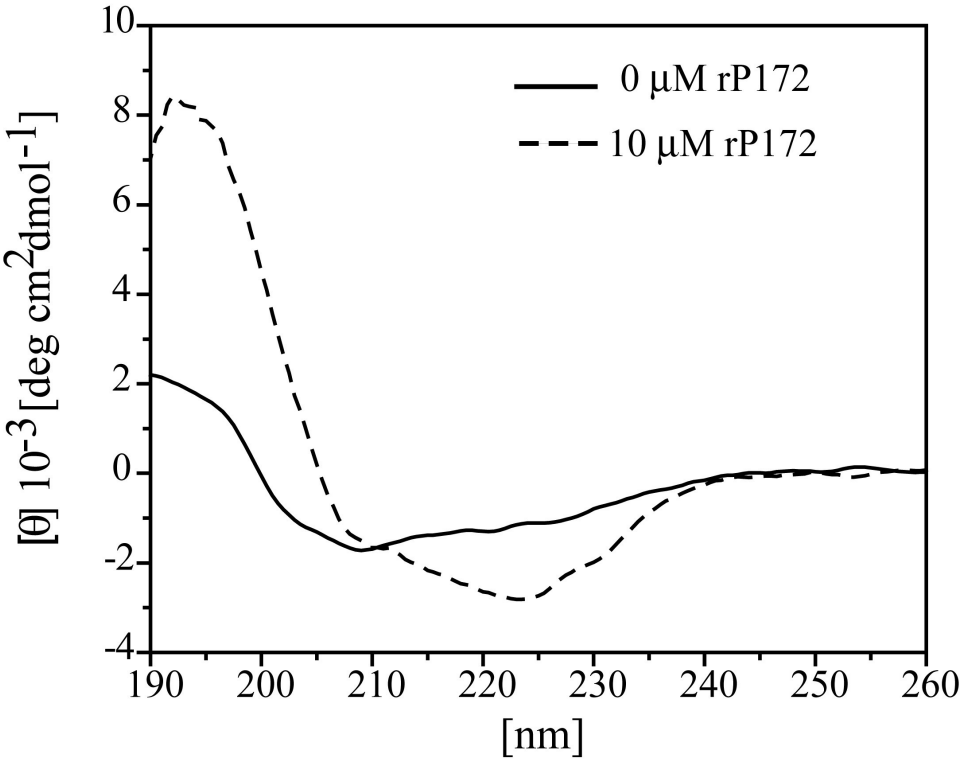

FIG 9

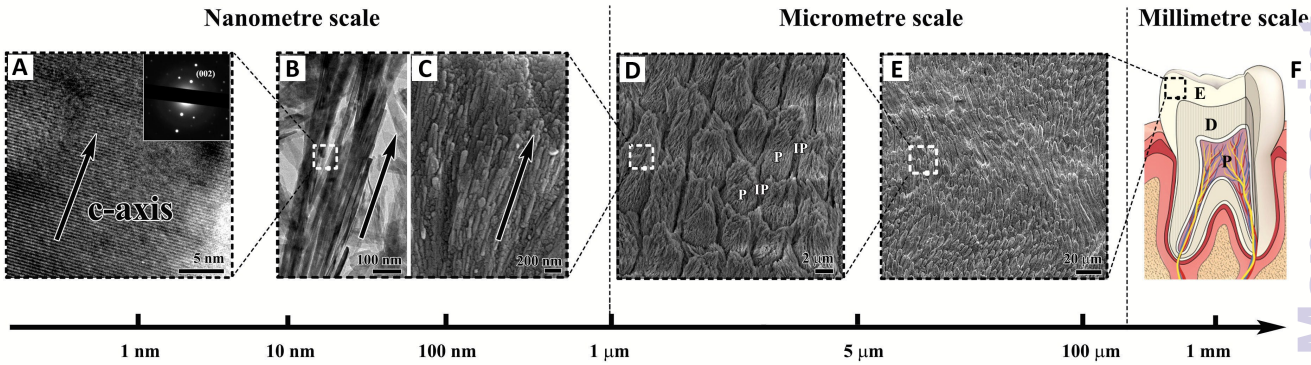

FIG 10

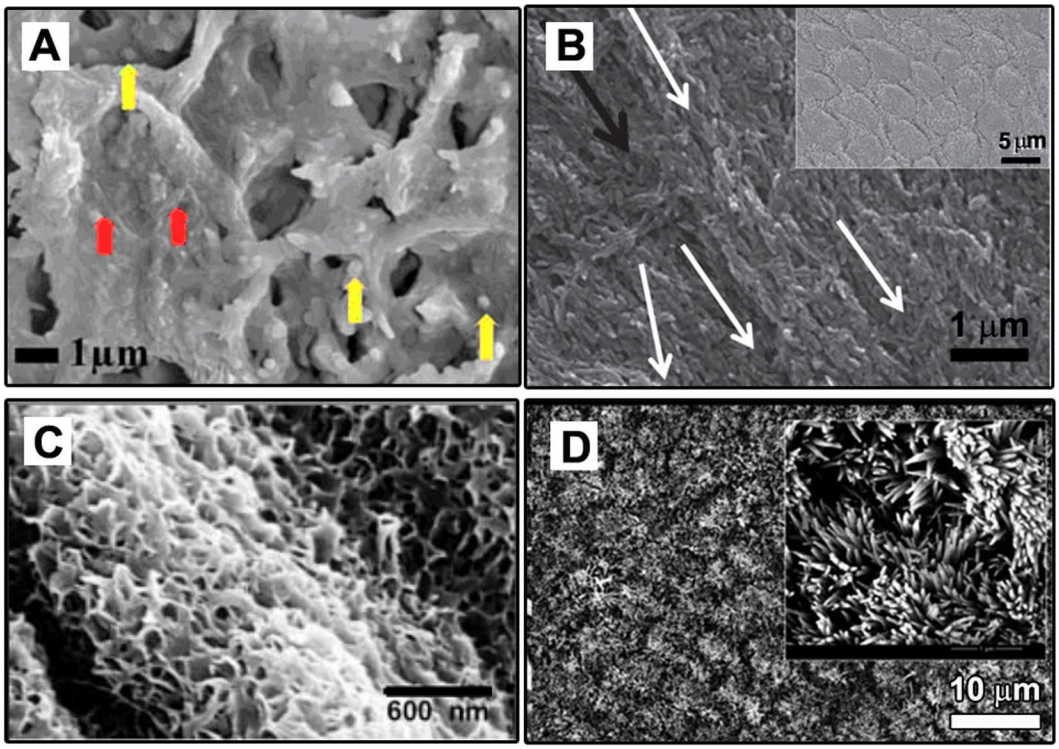

FIG 11

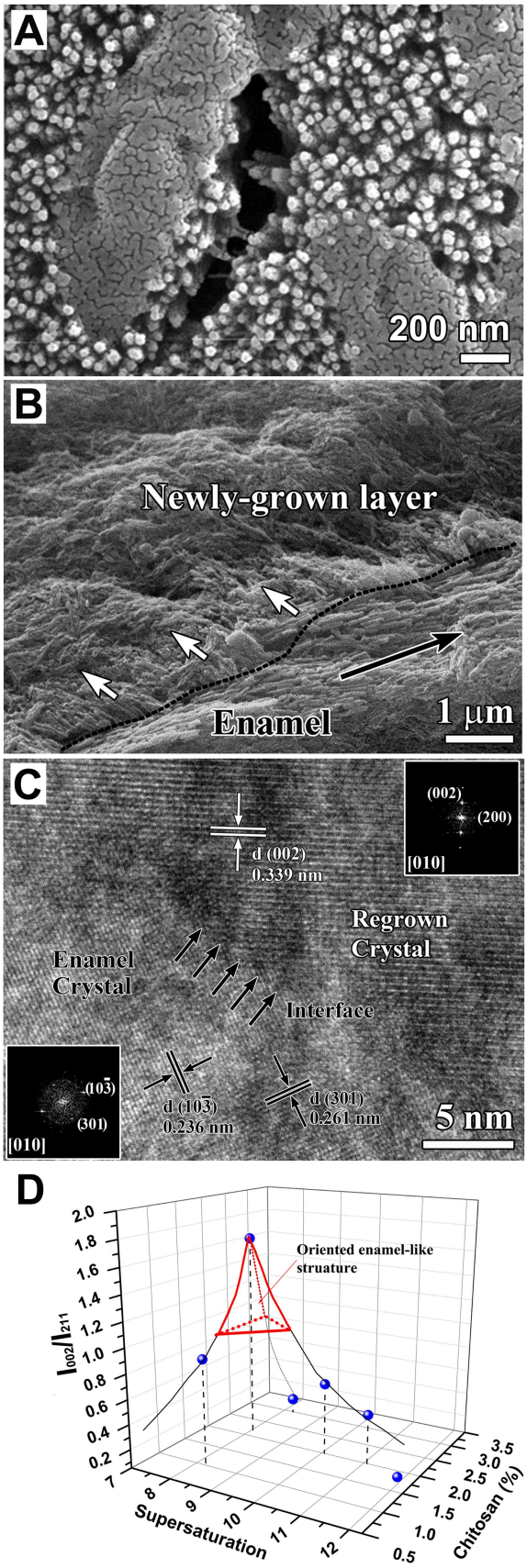

FIG 12

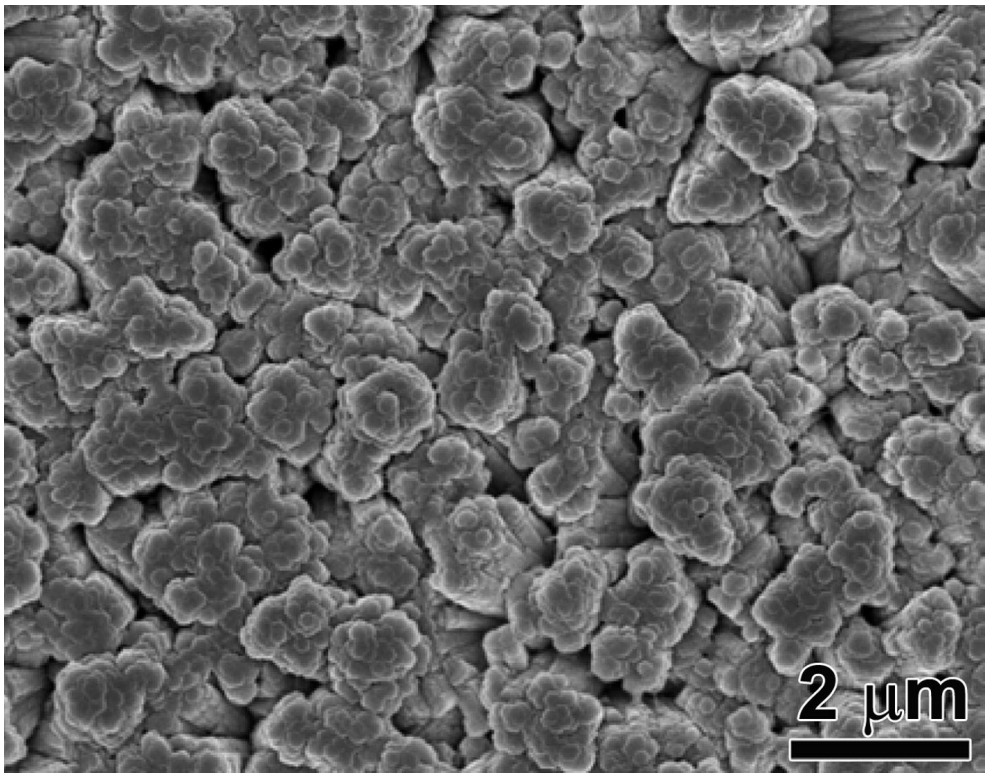

FIG 13

TOC

The importance of amelogenin in enamel formation, and its potential to be applied in biomimetic re-construction of human enamel are discussed.